République Algérienne Démocratique et Populaire
Ministère de l'Enseignement Superieur et de la Recherche Scientifique

Université Echahid Hamma Lakhdar d'El-Oued
FACULTE DE TECHNOLOGIE
DEPARTEMENT DE GENIE MECANIQUE

Présenté pour l'obtention du diplôme de

Mémoire de fin d'étude

MASTER ACADEMIQUE

Domaine: Sciences et Technologie
Filière: Génie mécanique
Spécialité: Energétique

Thème

Contribution to the Simulation of Coupled Transfers Phenomenon

Application on the PEM Fuel Cell

Présenté par

FERDJANI Abdelfettah

YAHIA Abdennour

Devant le jury composé de

ATTIA Mohammed El-Hadi	MCA	Président	UEHL El-Oued
REKBI Fares Mohammed Laid	MCB	Examinateur	UEHL El-Oued
ATIA Abdelmalek	MCA	Encadreur	UEHL El-Oued

2017-2018

Dedication

To our parents,

To our families,

To our friends

ACKNOWLEDGMENTS

We would like to thank to our supervisor. Dr. Abdelmalek Atia for his guidance, suggestions and comments. We also thank all staff of Mechanical Engineering Department for their information's and supports. We would also like to thank the lecturers who have been engaged in correcting our mistakes and working on our evaluation. In the last we express sincere thanks to our families for their support and for their understanding in every step of our education.

TABLE OF CONTENTS

LIST OF TABLES

LIST OF FIGURES

NOMENCLATURE

LATIN LETTERS

Symbol	Description	Unit
A	Electrode surface	m^2
a	Activity	_
b	Slope of Tafel	V
C_p	Specific heat	$J.kg^{-1}k^{-1}$
D	Coefficient of diffusion	$m^2.s^{-1}$
E	Standard potential of the reaction	V
F	Constant of Faraday	$96485C.mol^{-1}$
i	Current density	$A.m^{-2}$
$0\ i$	Exchange current density	$A.m^{-2}$
J	Volume density	$A.m^{-3}$
K	Permeability	m^2
k	Thermal conductivity	$W.m^{-1}k^{-1}$
M	Molar mass	$Kg.mol^{-1}$
n	Number of electrons exchanged during the reaction	_
P	pressure	Pa
R	Constant gas perfect	$8.314\ J.mol^{-1}k^{-1}$
S	Source term	$W.m^{-3}$
T	Temperature	K
V	Electric potential	V
U , v	Gas velocities	$m.s^{-1}$
x	Abscissa	m
y	Ordered	m
Y	Mole fraction	_

GREEK LETTERS

Symbole	*Description*	*Unit*
α	*Load transfer coefficient*	_
$\mathcal{E}$	*Porosity*	_
η	*Surge / voltage drop*	*V*
λ	*Moisture content of the membrane*	mol_{H_2O} /mol_{so_3}
μ	*Dynamic viscosity*	$Kg.m^{-1}\ s^{-1}$
ρ	*Density*	$Kg.m^{3}$
σ	*Membrane conductivity*	$S\ .m^{-1}$
ΔS	*entropy of the reaction*	$J\ .mol^{-1}.k^{-1}$

INDICES AND EXHIBITORS

0	Reference condition
A	Anode
act	activation
C	Cathode
CL,cl	Anode catalyst layer or cathode
Ch	channel
conc	Concentration
E	Entrance
eff	effective
G	Gas
GDL , gdl	Anode or cathode gas diffusion layer
I	specie
L	boundary
M	Membrane
ohm	ohmic
PB	Bipolar plate Abbreviation
PAC	Fuel cell
PEMFC	Proton Exchange Membrane Fuel Cell
SPEFC	Solid Polymer Electrolyte Fuel Cell
IEMF	CIon Exchange Membrane Fuel Cell
AME	Electrode Membrane Assembly "Membrane Electrode Assembly"
PTFE	Poly Tetra Fluoro Ethylene

GENERAL INTRODUCTION

Increasing levels of pollution and possible anthropogenic global warming resulting from the combustion of fossil fuels have urged scientists to consider alternative energy conversion and power generation systems that could satisfy the global energy demands in more environmental-friendly ways. Wind, tidal, solar and hydrogen based renewable energy systems are some of the potential areas in this regard. Hydrogen-based renewable energy systems such as fuel cells offer a promising pathway with the prospect of low- to zero-emissions during power generation for sub-watt to megawatt applications in transportation, manufacturing and communications.

The combination of high efficiency, environmental benefits and versatility make fuel cells a suitable power generation device for both terrestrial and space applications. Despite these potential benefits, the commercial deployment of fuel cells faces many challenges such as, high operating cost and a lack of existing hydrogen infrastructure

The fuel cell was first demonstrated by Lawyer-cum-inventor William Grove in 1839, but no further significant research was carried out in this field until the late 1940s . The first commercial application of a fuel cell was in space and military systems. Among the different types of fuel cells, the polymer electrolyte membrane (PEM) fuel cell is considered a promising approach due to its low operating temperature and simple design configuration. The basic operating principle of a fuel cell is simple, but involves the coupling of complex transport phenomena such as species transport by convection and diffusion, heat transfer, charge balance and electrochemical kinetics. These transport phenomena lead to certain efficiency losses in the fuel cell that affect its overall performance. The performance of a fuel cell can be investigated in two ways; either by experimental techniques or by numerical simulations. Experimental methods have limitations when investigating the complex interaction of transport phenomena taking place inside the fuel cell, whereas numerical modelling provides a better insight into the problem. Furthermore, it is not possible to perform detailed in-situ measurements of a fuel cell during its operation because of its reactive environment. The complex experimental setup of the fuel cell system has stimulated efforts to develop sophisticated numerical models of the fuel cell that can simulate and predict the coupled transport of reactant and product species, heat transfer and charge balance along the fuel cell domain.The present research focuses on computational fluid dynamics (CFD) based multi-physics numerical modelling of the coupled transport phenomena that occur in the PEM fuel cell. These numerical analyses have been carried out using two dimensional numerical modeling techniques.

This thesis is presented in the form of fourth chapters:

Chapter 1 presented a general introduction to fuel cells and their applications.

Chapter 2 provides an introduction to the working principals of fuel cells and thermodynamics law related to fuel cells system.

In chapter 3, the mathematical equations of different transfer phenomenon were established.

Chapter 4 presents a numerical simulation using CFD Analysis for gas flow in Gas Diffusion Layer zone

CHAPTER I

Fuel Cell Systems

Concepts and Description

I.1.Introduction

Fuel cells has attracted much attention as a potential power source for portable electronic devices, it is convert the chemical energy of hydrogen and oxygen directly into electricity. Their high efficiency and low emissions have made them a prime candidate for powering the next generation of electric vehicles, and their modular design and the prospects of micro-scaling them have gained the attention of cellular phone and laptop manufacturers. Their scalability makes them prime candidates for a variety of stationary applications including distributed residential power generation. The basic structure and operation principle the polymer electrolyte membrane (PEM) fuel cell considered here are illustrated in Fig. I.1. The polymer electrolyte consists of a per fluorinated polymer backbone with sulfonic acid side chains. When fully humidified, this material becomes an excellent protonic conductor. The membrane and the two electrodes (refloated porous carbon paper or cloth with platinum on supported carbon) are assembled into a sandwich structure to form a membrane-electrode assembly (MEA). The MEA is placed between two graphite bipolar plates with machined groves that provide flow channels for distributing the fuel (hydrogen) and oxidant (oxygen from air).The hydrogen-rich fuel is fed to the anode, where the hydrogen diffuses through the porous gas diffusion electrode (GDE). At the catalyst layer, the hydrogen splits into hydrogen protons and electrons according to:

$2H_2 \Rightarrow 4H+ + 4e-$ (I.1)

Driven by an electric field, the H^+ ions migrate through the polymer electrolyte membrane. The oxygen in the cathode gas stream diffuses through the gas diffusion electrode towards the catalyst interface where it combines with the hydrogen protons and the electrons to form water according to:

$O_2 + 4H+ + 4e- \Rightarrow 2H_2O$ (I.2)

The overall reaction is exothermic and can be written as:

$2H_2 + O_2 \Rightarrow 2H_2O$ + electricity + heat (I.3)

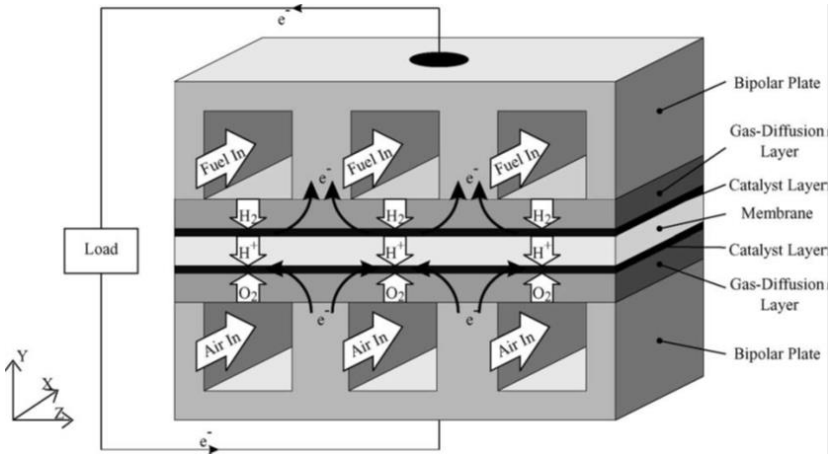

Figure. I.1. Schematic of a PEM fuel cell.[1]

I.2 Types of Fuel Cell

This is Different types of the fuel cell systems have been investigated by researchers to improve their performance and promote their commercialization. Currently, five classes of fuel cells have emerged as viable power systems for the present and near future applications. Each type of fuel cell has some merits and drawbacks. A brief description of the major types of fuel cells is presented in the following sections.

I.2.1 Polymer Electrolyte Membrane (PEM) Fuel Cell

The polymer electrolyte membrane (PEM) fuel cell is regarded as one of the most promising types of fuel cells due to its simplicity and low operating temperature. This type of fuel cells generally operate between 50 to 100 °C, which makes them suitable for automotive and mobile applications [1].In this type of fuel cells, the electrolyte is a solid polymer which contains mobile protons. The major drawback of the low operating temperature of PEM fuel cells is the low electrochemical reaction rate, which can be addressed using sophisticated catalysts and electrodes.

I.2.2 Alkaline Fuel Cell

The alkaline fuel cell is one of the most developed types of fuel cells which was used by NASA moon missions in the late 1960s [1]. This type of fuel cells produces power through a ‘redox’ reaction between hydrogen and oxygen. The anode and cathode are separated by a porous matrix saturated with an aqueous alkaline solution of potassium hydroxide (KOH). Pure oxygen reacts with the potassium hydroxide to make potassium carbonate as a by-product. This potassium carbonate causes a blockage of pores that slowly reduces the performance of this type of fuel cells.

Alkaline type fuel cells operate at fairly high temperatures ranging between 50 to 200 °C and they have higher efficiency when compared to the PEM fuel cells. Alkaline fuel cells also have an edge over PEM fuel cells due to their low activation over potential at the cathode, but conversely they need pure hydrogen and oxygen to achieve optimum performance which makes their operation costly [1], [2]

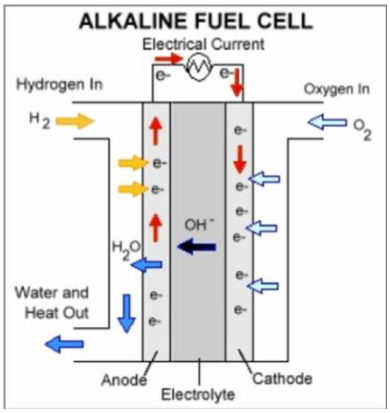

Figure I.2: Operating principle of alkaline type fuel cells[2]

I.2.3 Phosphoric Acid Fuel Cell

This type of fuel cells uses liquid phosphoric acid as an electrolyte. Hydrogen is introduced at the anode side and is oxidized to produce positively charged protons and negatively charged electrons. The ionic conductivity of the phosphoric acid is low at low temperatures. Furthermore, it solidifies at temperatures below 40 °C, which makes the initial start-up difficult and restricts the continuous operation of this type of fuel cells [51]. Phosphoric acid fuel cells operate at a temperature of around 220 °C and can tolerate carbon monoxide, which is not acceptable for many other types of fuel cells. Moreover, In this type of fuel cells, the hydrogen fuel problem can be solved by reforming natural gas (CH4, methane) to hydrogen and carbon dioxide, but the equipment required for this adds considerable cost, complexity and size to the fuel cell system [2].

I.2.4 Solid Oxide Fuel Cell

Solid oxide fuel cells are made up of four layers, three of which are ceramic. Ceramics do not become ionically active until they reach at very high temperature and therefore the solid oxide fuel cell is only operational in the region of 800 – 1200ºC. Oxygen gas enters at the cathode side while fuel enters at the anode side. Light hydrocarbon fuels such as methane, propane and butane are mostly used as fuels in this type of fuel cell. Oxygen is reduced into oxygen ions at the cathode side. These oxygen ions then diffuse through the solid oxide electrolyte to the anode where they electro-chemically oxidize the fuel.

This type of fuel cell is generally suitable for large industrial applications because of its high operating temperature range. Due to such high temperatures, a fast reaction rate can be achieved without using any expensive catalysts.

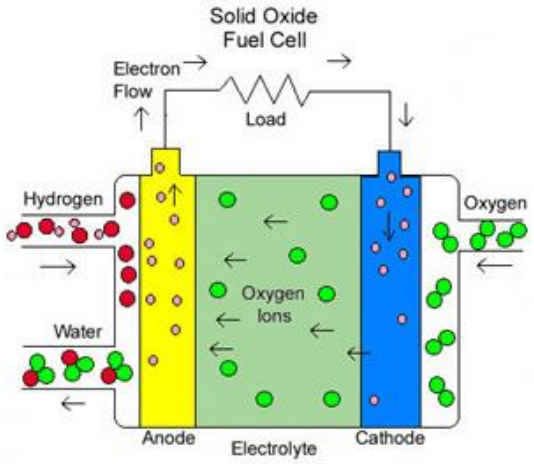

Figure I.3: Operating principle of solid oxide fuel cells[2]

I.2.5 Molten Carbonate Fuel Cell

The electrolyte of a molten carbonate fuel cell is a mixture of molten alkali metal carbonates, usually a binary mixture of lithium and potassium, or lithium and sodium carbonates. To melt the carbonate salts and achieve high ion mobility through the electrolyte, this type of fuel cell operates at around 650 °C [52]. Due to the high temperatures, the alkali carbonates form a highly conductive molten salt with the carbonate (CO3-2)ions, providing ionic conduction [1].Unlike other types of fuel cells, molten carbonate fuel cells do not require any external reformer to extract hydrogen from energy-dense fuels. Due to the high operating temperature, the fuels are converted into hydrogen within the fuel cell itself by internal reforming.

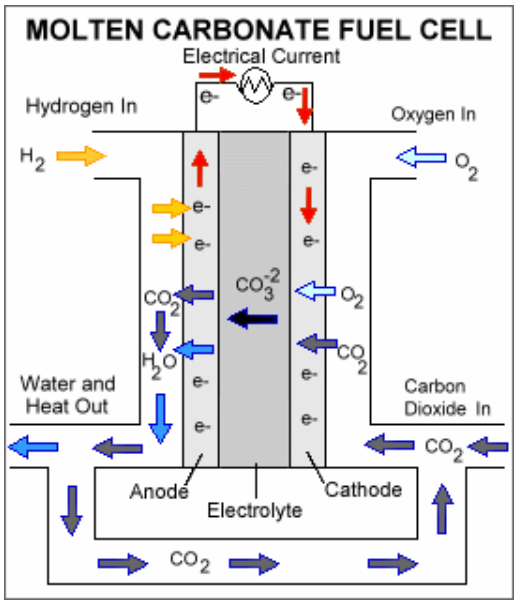

Figure I.4: Operating principle of molten carbonate fuel cells[1]

I.3 Research on Proton Exchange Membrane Fuel Cell

A lot of research has been done on various aspects of PEM fuel cells. The standard single PEM fuel cell is a combination of two endplates as current collectors, two gas diffusion layers, two catalyst layers and a proton exchange membrane

Generally, the hydrogen is fed in from anode side channel and split in the catalyst layer into protons and electrons. The protons pass through the membrane to the cathode catalyst where they combine with the oxygen fed in from the cathode-side channel and electrons from the external electric circuit to form water. The movement of the electrons in the external circuit is the current generated.

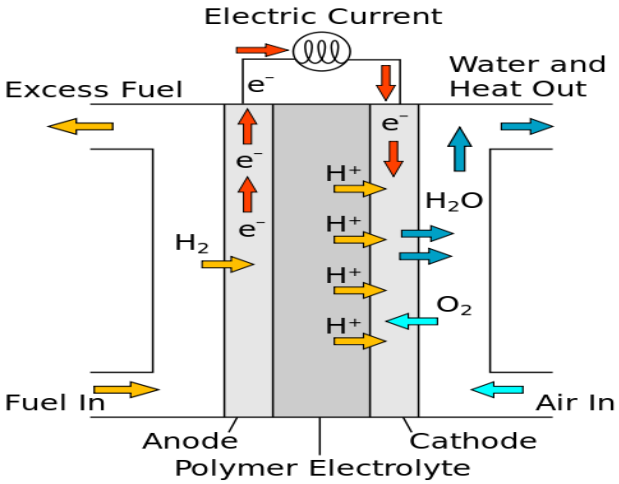

Figure I.5: Schematic of a PEM fuel cell showing the main reactions (Mattuci 2001)[1]

I.4 PEM Fuel Cell: Description

Polymer electrolyte membrane (PEM) fuel cells are a relatively new technology within the fuel cell community. This type of fuel cell was first developed by General Electric in the USA in the 1960s for use by NASA on its manned space vehicles [3].The development of PEM fuel stagnated in the 1970s and early 1980s. However, in the second half of the 1980s there has been are naissance of interest in this type of fuel cell. Rapid development during the past decade has now brought the PEM fuel cell significantly closer to commercial reality.

PEM fuel cells consist of three major components: a negatively charged electrode (cathode), a positively charged electrode (anode) and a membrane electrode assembly. The membrane electrode assembly consists of a current collector, a porous gas diffusion layer, a catalyst layer and an electrolyte membrane. The operating principle of a PEM fuel cell is simple and can be considered to be the opposite of electrolysis. In electrolysis, an electric current is passed through water to produce hydrogen and oxygen, whereas in a PEM fuel cell, hydrogen and oxygen gases are passed at either side of the polymer electrolyte membrane where hydrogen is split into its elementary constituents - the positively charged proton ions and the negatively charged electrons.

The potential difference between anode and cathode attracts the protons from anode to cathode causing them to travel through the electrolyte membrane, whereas the electrons travel first through an external circuit and then to the membrane catalyst layer interface at the cathode side where they react with the reduced oxygen atoms, following this, the reduced oxygen atoms react with the protons diffusing through the membrane to produce heat and water as by-products [4].The electrochemical reactions for the PEM fuel cell can be stated as follows:

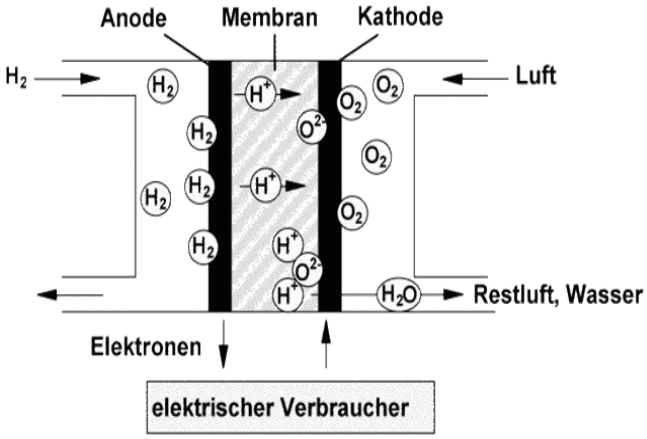

Figure I-6: Schematic view of a PEM fuel cell and its operating principles[4].

Anode Reaction:

$2H_2 \Rightarrow 4H^+ + 4e^-$ (a)

Cathode Reaction:

$O_2 + 4H^+ + 4e^- \Rightarrow 2H_2O$

Overall Reaction:

$2H_2 + O_2 \Rightarrow 2H_2O$ (c)

The following figure explains the basic operating principles of the PEM fuel cell and highlights its important components.

I.4.1 the differences between the two PEMFC variants

A variant of the PEMFC which operates at elevated temperatures is known as the high temperature PEMFC (HT PEMFC). By changing the electrolyte from being water-based to a mineral acid-based system, HT PEMFCs can operate up to 200 °C. This overcomes some of the current limitations with regard to fuel purity with HT PEMFCs able to process reformate containing small quantities of Carbon Monoxide (CO). The balance of plant can also be simplified through elimination of the humidifier.

HT PEMFCs are not superior to low temperature PEMFCs; both technologies find niches in where their benefits are preferable. The table below summarizes differences between the two PEMFC variants:

	Low Temp. PEMFC	High Temp. PEMFC
Operating temperature	80-100 degrees C	Up to 200 degrees C
Electrolyte	Water-based	Mineral acid-based
Pt loading	0.2-0.8 mg/cm^2	1.0-2.0 mg/cm^2
CO tolerance	<50 parts per million	1 - 5 % by Volume
Other impurity tolerance	Low	Higher
Power density	Higher	Lower
Cold start?	Yes	No
Water management	Complex	None

The table I.1. The differences between the two PEMFC variants[4]

I.5 PEM Fuel Cell Components

A PEM fuel cell consists of four major components. The following sections briefly describe these components and their role in the operation of the fuel cell.

I.5.1 Polymer Electrolyte Membrane

The polymer electrolyte membrane is the heart of a PEM fuel cell. It has two main functions; firstly, it works as a gas separator, preventing the reactant gases from directly reacting with each other; secondly, it acts as the proton conductor. Typically, the electrolyte membrane consists of a Perfluroinated polymer backbone with Sulphonyl acid side chains [5].Nafion® membranes by Du-Pont are typically used as the de-facto standard for most of the polymer electrolyte fuel cells.

However, there are also other variants of electrolyte membranes, such as Flemion® and Aciplex® membranes, which are well known in the fuel cell industry [4], [6],[7]. Membranes have to be hydrated so as to sustain their protonic conductivity. It is therefore necessary for the membrane to retain a certain amount of water content so as to maintain its ability to transfer protons. This depends on two phenomena; firstly, that of the chemical affinity for water in hydrophobic regions of the membrane, which enables the membrane to absorb and retain water; secondly, that of the electro-osmotic drag phenomena, whereby each hydrogen ion is accompanied by one or two molecules of water [7], [8]. The requirement to keep the membrane hydrated restricts PEM fuel cell operation at higher temperatures. In general, to achieve high efficiency, the membrane must possesses the following properties [9], [10]

a) High proton conductivity to support high currents with minimum resistive losses and zero electronic conductivity.

b) Adequate mechanical strength and durability.

c) Chemical stability under operating conditions.

d) Extremely low fuel or oxygen by-pass to minimize crossover current.

e) Reasonable production cost which is compatible with intended application.

I.5.2 Gas Diffusion Layer (GDL)

The gas diffusion layer enables efficient distribution of the reactant and product species along the fuel cell domain. The gas diffusion layer is made up of a sufficiently porous and electrically conductive material. Materials of a typical gas diffusion layer include carbon paper or carbon cloth with typical thicknesses of 100- 300 μm [11]. The GDL is intentionally porous to increase the wetted surface area by hundreds and even thousands times the geometric surface area [3], [4]

The gas diffusion layer is characterized by its thickness, hydrophobic nature and dry resistance to flow and electric properties [12]. Performance of the PEM fuel cell is immensely influenced by the reactant/product species distribution along the gas diffusion layer since it can lead to issues such as water flooding and poor concentration distribution. To facilitate excess water removal from the fuel cell and minimize water flooding, the hydrophobicity of the GDL is increased by impregnating it with a hydrophobic material. The amount of hydrophobic agent used is a sensitive parameter as excess impregnation can result in the blockage of surface pores and thus a reduction of the GDL porosity [13]

I.5.3 Catalyst Layer

A fine layer of catalyst, usually the noble metal platinum (Pt), is applied to both faces of the electrolyte membrane. A catalyst loading of 0.1-0.3 mg/cm2 per membrane catalyst layer is typically used. The thickness of the catalyst layer is usually in the range 5-15 μm [14]. Due to the high cost of platinum, it must be used sparingly in order to reduce the overall cost of the PEM fuel cell [15].The catalyst layer breaks the bonds between the atoms of the reactant species and promotes higher reaction rates. At the anode side, the hydrogen molecules are absorbed onto the surface of the catalyst and the bonds between the hydrogen atoms are stretched and weakened so that they eventually break. A similar mechanism occurs on the cathode side where the reduction of oxygen is promoted by the action of the catalyst [7].

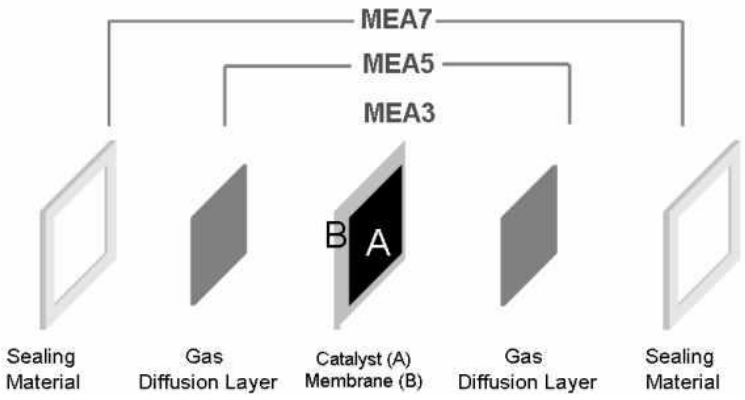

Figure I.7: The Image of fuel cell catalyst[7]

I.5.4 Bipolar / End Plates

The interconnection between the fuel cells in a stack is achieved using conductive plates. When machined on both sides, they are normally called bipolar plates. Plates which are fitted at the edges of the fuel cell stack and are machined on one side only are termed end plates. The term electrode plates will be used here to refer to the bipolar and end plates. [7]. These plates are an important component of any fuel cell system because they assist the supply of fuel and oxidant to the reactive sites, remove reaction products, collect produced current and provide structural support [16]. Conventionally, when the electrode plates are made of graphite; they constitute around 60 % of the total weight, 30% of total cost and 80% of the total volume of a fuel cell; the weight and cost of a fuel cell can be reduced significantly by improving the design of these plates. The essential requirements for the electrode plates are [11].

- ✓ High values of electronic and thermal conductivity;
- ✓ High mechanical strength;
- ✓ Impermeability to reactant gases;
- ✓ Resistance to corrosion;
- ✓ Low cost of production.

Bipolar plates are usually constructed from graphite. However, graphite is porous, fragile, and needs to be thick for the required strength, leading to an increase in weight, size and cost. As such, alternative materials have been under intense study by various researchers [17]-[18] Different design topologies, i.e. straight, serpentine or spiral shapes have been used by the researchers to achieve the

aforementioned functions efficiently with the aim of obtaining high performance and economic advantages. Around a 50% increase in fuel cell performance has been reported just by improving the distribution of the gas flow fields [19]. Bipolar/end plates typically have fluid flow channels stamped on their surfaces. Flow channel geometry at both the anode and cathode sides can be different from each other depending on their design requirements. The essential requirements for the bipolar plates with respect to physio-chemical characteristics are the uniform distribution of the reactant species over the active surface of the electrode to minimize the concentration over potential. The choice of flow field configuration strongly affects the performance of a PEM fuel cell, especially in terms of water management and distribution of reactant species. Due to this, the effective design and optimization of the gas flow fields and the bipolar plates remains a very important issue for cost reduction and performance improvement of the PEM fuel cell. The different types of flow field configurations that have been used by researchers are discussed in the following sections.

I.5.4.1 Serpentine Shaped Gas Flow Channel

The serpentine shaped gas flow channel configuration is a common option for many fuel cell designers. In this design configuration, only one flow path exists for the reactant gases across the flow field plate and any liquid water accumulating in the channel is quickly pushed out of the cell. Watkins et al. [20] studied the optimization of serpentine shaped flow channels. This type of flow field configuration results in high pressure losses and therefore needs a high pressure flow.

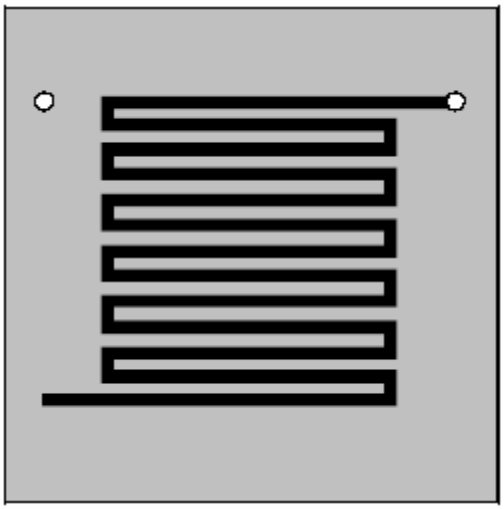

Figure I.8: Serpentine shaped gas flow channel configuration[20]

I.5.4.2 Parallel/Straight Shaped Gas Flow Channel

Pollegri et al. [16] introduced the concept of a parallel/straight type gas flow channel configuration. This type of flow field has an advantage over the serpentine shaped channels due to the lower pressure losses; on the other hand, a major drawback is that different paths exist across the bipolar plate for the reactant gases, potentially causing ineffective water removal because of the uneven flow distribution of the reactant flow through the fuel cell domain.

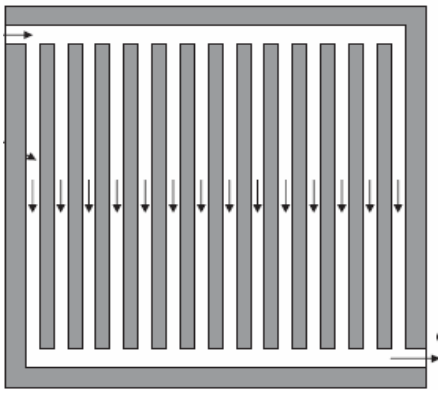

Figure I.9: Parallel gas flow channel configuration[16]

I.5.4.3 Discontinuous Type Gas Flow Channel

The discontinuous type gas flow channel configuration has been proposed as a solution to the problem of low diffusion rates along the gas diffusion layer in a fuel cell. Discontinuity of the gas channel passively forces the reactant species to diffuse along the gas diffusion layer and facilitates the removal of water. In this type of flow channel configuration, the transport of the reactant species in the gas diffusion layer is forced instead of relying on free convection [21]

I.5.4.4 Spiral Shaped Gas Flow Channel

Kaskimies et al. [19]proposed a spiral shaped gas flow field configuration. This configuration combines the effective water removal of the single channel geometry with the advantage of having channels containing fresh and depleted cathode gas side by side, leading to better distributions of oxygen and water. However, the manufacturing cost of this type of flow field configuration is significantly higher.

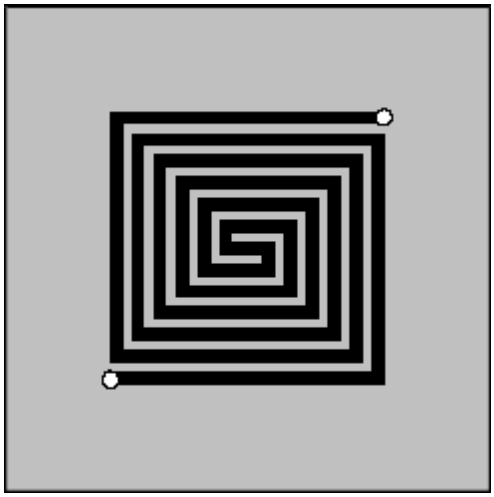

Figure I.10: Spiral flow field configuration[19]

I.6 Conclusion

This chapter reviewed the existing literature on PEM type fuel cells, mainly focusing upon the important components and transport phenomena taking place inside its domain. In this chapter, Different materials for bipolar/end plates were also discussed in this chapter. It was described that stainless steel is used as a material for the gas distributor and bipolar plates due to lower required thickness, good mechanical strength and cost effectiveness.

CHAPTER II

Working principles of the Fuel cell

II.1 Introduction

The purpose of this chapter is to present the necessary knowledge on the fuel cell (PEM) in order to clarify the structural notions of our main topic of study. We begin with a description of the physicochemical phenomena in a PEM fuel cell. The main issues related to water management are exposed. Finally, a state of the art modeling work is presented in order to make our contribution as clear as possible.

II.2 Physico-chemical phenomena in a PEM fuel cell

Although the operating principle of the PEM is simple, the phenomena that occur in the cell core are numerous. We have fluidic, electrochemical, thermal phenomena as well as water transport. The interaction between these various strongly coupled phenomena is important for the proper functioning of the system.

II.2.1 Fluidic phenomena

- **charge losses**: Gases injected into the distribution channels of the plates

bipolar, suffer a loss of pressure resulting in a pressure drop inside the channels. This pressure loss depends mainly on the geometric design of the channels. The geometry of the channels is particularly important to ensure a homogeneous distribution of gases over the entire surface of the electrode while minimizing charge losses. Thus, the partial pressure of the gases is generally less than the total gas pressure set at the inlet of the cell. Nevertheless, these hydraulic phenomena have not been taken into account in this thesis: the pressure drops are in particular supposed to be weak and therefore neglected.

- **Gas Diffusion Layer** : During their circulation in the channels, the gases diffuse towards the electrodes through the diffusion layers following the first law of Fick :

$$\vec{j} = - D \overrightarrow{grad}\, C \qquad (II.1)$$

j is the diffusion flux of the gases, C being the concentration and D the diffusion coefficient of the gases. This law states that the flow of matter is locally controlled by the gradient of concentration. This behavior tends to soften all the variations of the concentration C because the particles always move from a place of high concentration to a place of lower concentration.

the quantity of matter is generally conserved, one can write the following conservation law:

$$\frac{\partial C}{\partial t} + \overrightarrow{grad}\, j = 0 \qquad (II.2)$$

by introducing the first law of Fick in this equation, we obtain the diffusion equation, also called the second law of Fick:

$$\frac{\partial C}{\partial t} = Ddiv(\overrightarrow{grad\, c}) \qquad (II.3)$$

for one dimension, the diffusion equation is simply given by:

$$\frac{\partial C}{\partial t} = D\frac{\partial^2 C}{\partial x^2} \qquad (II.4)$$

the principle of the fundamental law of thermodynamics applies to gases which are supposed to be perfect. This principle gives the relation between the pressure of the gas P, its volume V, its temperature T and the number of moles N:

$$PV=NRT \qquad (II.5)$$

This relation can also be written as a function of the concentration C of the gas in the form:

$$P = \frac{NRT}{V} = CRT \qquad (II.6)$$

II.2.2 Thermal phenomena

the role of thermal phenomena plays an important role in PEMFC. Indeed, temperature is a decisive parameter for chemical reactions: the higher the temperature, the greater the kinetics of the reactions. The electrolyte must be hot enough to be a good ionic conductor. However, to ensure correct operation of the battery, it is necessary to work below a certain temperature (depending on the type of battery) to prevent drying of the membrane. the exothermic reaction between hydrogen and oxygen is the main source of heat. Other elements contribute to the internal heating of the cell, such as the electric current that heats the conductive components of the cell and the degree of humidification of the electrolytic membrane [22] The heat produced at the level of the active layers is decomposed into a heat flux passing through the electrodes and another flow through the membrane by the phenomena of conduction and material transport. A significant amount of the heat produced is removed at each component (bipolar plate, diffusion layer, electrode, membrane) by the phenomena of convection and evaporation of water. The evacuated heat flow is influenced by both the external cooling temperature and the flow rate of the water produced or injected.

origin of terms used in the literature are different depending on the assumptions of simplifications, the layer considered and the taking into account of the liquid phase (phase change) or not.

The different terms of thermal energy sources used in the literature are given in **Table II.1.**

The source terms consist of two parts:

Channel	"GDL" diffusion layer	Catalyst Layer "CL"	Membrane	Bipolar plates	References
$S_T = 0$	0	$i = \left(\eta + T\frac{dv_{oc}}{dt}\right) + \frac{i^2}{\sigma_m}$	$\frac{i^2}{\sigma_m}$	0	[23]
0	$\varepsilon_g \beta(T_s - T_g)$	$\left[\frac{T(-\Delta S)}{nF} + \eta_c\right] i_c$	$\frac{i^2}{\sigma_m}$	0	[24]
0	$\varepsilon_g \beta(T_s - T_g)$	$\left[\frac{T(-\Delta S)}{nF} + \eta_c\right] i_c$	0	0	[25]
$r_{w\,h_l}$	$\frac{i^2}{\sigma_s^{eff}} + r_{w\,h_l}$	$\eta R_{an,cat} + i^2\left(\frac{1}{\sigma_s^{eff}} + \frac{1}{\sigma_m^{eff}}\right) + r_{w\,h_l}$	$\frac{i^2}{\sigma_m^{eff}} + r_{w\,h_l}$	$\frac{i^2}{\sigma_s}$	[26]

Table II.1*: Expressions of terms "ST" heat sources.*

Reversible: corresponding to the half-reactions of oxidation of hydrogen and reduction of oxygen, because of the difficulties of evaluation of the standard entropy of the ions and since only the entropies of the reactions are the measurable magnitudes It is accepted by convention that hydrogen has a standard enthalpy of formation and a Gibbs enthalpy of zero. This justifies the hypothesis that the oxidation of hydrogen at the anode does not lead to the release of heat and the reduction of oxygen at the cathode is the sole source of the heat source of reaction (creation of entropy linked to the global reaction).

Irreversible: associated with the overvoltages at the electrodes, and finally a part corresponding to the phenomena of sorption of the water in the membrane. This is the only source that depends on the mass balance, not on the electrical regime.

II.2.2.1 Sorption of water

The liquid water appears in the fuel cell when the pressure of the water vapor reaches its saturation value at the operating temperature of the cell. On the contrary, the liquid water is evaporated when the pressure of the water vapor is lower than its saturation value.

The phase change process (condensation / evaporation) (Equation II. 7) is also an important factor in determining the presence of liquid water in the multiphasic model

$$S_T = r_w h_l \qquad (II.7)$$

Where hl: enthalpy of formation of water vapor in (N.m. kg^{-1}). The expression of phase change rate (condensation / evaporation) "r_w" is given in equation (II.8):

$$r_w = c_r \, max\left(\left[(1-s)\frac{P_{H2O}-P_{Sat}}{RT}M_{H2O}\right],\left[-s\rho_L\right]\right) \qquad (II.8)$$

c_r: condensation rate is defined as: $c_r = 100 / S$.

Another term of heat source term was used by [24], [25] (equation II.9) in the gas diffusion layer, represents the heat exchange to and from the solid matrix of GDL.

$$S_T = \varepsilon_g \beta\left(T_s - T_g\right) \qquad (II.9)$$

Where ε_g: porosity of GDL, β: is a modified heat transfer coefficient that takes into account the convective heat transfer in (W / m^2) and the specific surface (m^2 / m^3) of the porous medium [24]Therefore, the unit of β is (W / m^3).In our case, the variation of the mass flow of water due to condensation / evaporation is not considered. Thus, the choice of source terms for modeling is discussed in the next chapter.

II.2.2.2 Electrochemical activation of reactions

reactions The irreversibility of electrochemical reactions results in overvoltages at the electrodes, which reduce the electrical efficiency of the battery. The writing of the Butler-Volmer law modeling reaction activation phenomena or the modeling of coupled mass and charge transfers at the level of the electrode makes it possible to estimate the corresponding heat sources.

$$S_{T=\eta\, i} \qquad (II.10)$$

η : Activation overvoltage in (V) in both sides anode and cathode

II.2.2.3 Joule effect

The Joule effect is caused by the proton transfer resistance in the membrane (the ohmic resistance of the solid zones). The expression associated with the Joule effect is given in equation (II.11).

$$S_T = \frac{i^2}{\sigma_m} \quad (w/m^3) \qquad (II.11)$$

With i: the current density in the cell in (A / m^2), σ : Proton conductivity of membrane or electrical in the electrodes (S / m).

II.2.2.4 Entropy of half-reactions

reactions Half-reactions at the electrodes cause a reversible release of heat. Their expression in equation (II.12).

$$S_T = \frac{T(-\Delta S)}{nF} i_c \qquad (II.12)$$

ΔS : Specific entropy (J / mole K).

II.2.3 Electrochemical phenomena

Catalyst Layer. It is in this zone that the reaction mechanism of the two oxidation-reduction half-reactions is applied, thereby transforming the chemical energy into electrical energy. During this transformation, losses due to the chemical kinetics of the reactions appear. The condition necessary for the reaction mechanism is the bringing together at the same point of the reactive gas, the proton, the electrons and the catalyst. This place is called the place of "triple contact" or "triple phase". The active layer of the electrode has little hydrophobicity. It is generally considered drowned [27]Thus, it causes a resistance to the progression of the gas as in the diffusion layer. Consequently, the theoretical electrochemical potential E given by equation (II.13) undergoes a voltage drop caused by the electrochemical losses.

$$E = E^0 + \frac{RT}{nF} Ln \left(\frac{PH2 \sqrt{(P)_{O_2}}}{P_{H2O}} \right) \qquad (II.13)$$

ideal standard potential

$E^0 = 1.1V$	[29] [28] [30, 31]
$E^0 = 0.0025T + 0.2329$	
$E^0 = 1.23 - 0.9 \times 10^{-3} (T - 298) + 2.3 \frac{RT}{4F} (P_{H2}^2 P_{O2})$	[23] [33][32]
$E^0 = 1.229 - 0.83 \times 10^{-3} (T - 298.15) + 4.31 \times 10^{-5} T [Ln\ P_{H2} + Ln\ P_{O2}]$	[34-36]

II.2.3.1 The loss of activation

Its expression is given by the law of Tafel , which shows a logarithmic relationship with the current density i:

$$V_{act} = \frac{RT}{\alpha nF} Ln\left(\frac{i}{i_0}\right) \qquad (II.14)$$

Where i_0 is the exchange current density which represents the minimum value provided by the battery ($i > i_0$).

II.2.3.2 Ohmic losses

Under Ohm's law, their expression is given by [32], [37]

$$V_{ohm} = RI \qquad (II.15)$$

Where R is the equivalent ohmic resistance. It is equal to the sum of the electrical resistances of the anode Ra, the cathode R_c and the membrane R_m ($R = R_a + R_c + R_m$).

II.2.3.3 The loss of concentration

Concentration overvoltages then result in the appearance of a limit current where the reagents are no longer sufficient to feed the reaction. For this current value, the potential of the electrode vanishes quickly. The loss of concentration is given by the following equation:

$$V_{conc} = \frac{RT}{\alpha nF} Ln\left(1 - \frac{i}{i_L}\right) \qquad (II.16)$$

Where i_L is the limit current density. It represents the maximum value that the battery can provide before undergoing a voltage drop when saturation of the concentration on the cathode side.

The expressions for the concentration overvoltages are summarized in Table II.2.

Concentration surges	References
$V\ conc.c = \frac{RT}{2F} Ln\left(1 - \frac{i_c}{i_{L,c}}\right), i_{L,c} = \frac{2FD_{O2}\,C_{O2}}{\delta_{GDL}}$ $V\ conc.a = \frac{RT}{2F} Ln\left(1 - \frac{i_a}{i_{L,a}}\right), \quad i_{L,a} = \frac{2FD_{H2}\,C_{H2}}{\delta_{GDL}}$	[34-36]

Table II.2: Expressions of concentration overvoltages

II.3 Thermodynamics of Chemical Reactions

II.3.1 Free Energy Change of Chemical Reactions

Consider the chemical reaction below;

$$aA + bB \rightarrow cC + dD \qquad (II.17)$$

The change in Gibbs function of reaction, or Gibbs free energy of the reaction, under Constant temperature and pressure, is given by the equation

$$\Delta G = c\ \mu_C + d\ \mu_D - a\ \mu_{CA} - b\ \mu_B \qquad (II.18)$$

where μ is the chemical potential of the species. The maximum network obtainable from a chemical reaction can be calculated by the free energy change of the chemical reaction, the free energy change of a chemical reaction is given by

$$\Delta G = \Delta H - T\Delta S \qquad (II.19)$$

II.3.2 Standard Free Energy Change of a Chemical Reaction The chemical

potential of any substance may be expressed by an equation of the form

$$\mu = \mu_o + RT\ ln\ a \qquad (II.20)$$

where a is the activity of the substance and μ has the value μ° when a is unity. The standard free energy change ΔG° is given by

$$\Delta G^0 = c\mu_{C^0} + d\mu_{D^0} - a\mu_{A^0} - b\mu_{B^0} \qquad (II.21)$$

where $\mu_C^{\ o}$ indicates the standard chemical potential of product C, and so on. Substituting Eqs.2.48 and (II.18) into Eq.(II.21) yields

$$\Delta\ G\ = \Delta G^0\ +\ RT\ ln\frac{a_C^c\ a_D^d}{a_A^a\ a_B^b} \qquad (II.22)$$

Hence, the standard free energy change of a chemical reaction is

$$\Delta G^0 = \Delta\ G - \ RT\ ln\frac{a_C^c\ a_D^d}{a_A^a\ a_B^b} \qquad (II.23)$$

Assuming a process at constant temperature and pressure at equilibrium , since the free energy change for this process is zero, Eq (II.23) becomes

$$\Delta G^0 = -RT\ ln \frac{a_{C,eq}^c\ a_{D,eq}^d}{a_{A,eq}^a\ a_{B,eq}^b} = -RT\ ln\ K \qquad (II.24)$$

where the suffixes eq in the activity terms indicate the values of the activities at equilibrium, and K is the equilibrium constant for the reaction.

The importance of the knowledge of $\Delta G°$ is that it allows ΔG to be calculated for any composition of a reaction mixture. Knowledge of ΔG indicates whether a reaction will occur or not. If ΔG is positive, a reaction cannot occur for the assumed composition of reactants and products. If ΔG is negative, a reaction can occur. [38]

II.3.3 Relation Between Free Energy Change in a Cell Reaction and Cell Potential

The enthalpy change of any reaction, assuming constant temperature and pressure, can be showed as follows :

$$\Delta H = \Delta E + P\Delta V = Q - W\ P\Delta V \qquad (II.25)$$

If the reaction is carried out in a heat engine, then the only work done by the system would be the expansion work,

$$W = P\Delta V \qquad (II.26)$$

Hence Eq (II.24)becomes;

$$\Delta H = Q \qquad (II.27)$$

If the same reaction, which is under consideration is carried out electrochemically, the only work done by the system will not be the expansion work of the gases produced, but will also be the electrical work due to the charges being transported around the circuit between the electrodes. The maximum electrical work that can be done by the overall reaction carried out in a cell, where $Vrev,c$ and $Vrev,a$ are the reversible potentials at the cathode and anode respectively, is given by

$$We,max = ne(V\ rev,c - V\ rev,a) \qquad (II.28)$$

In the cell, n electrons are involved and the cell is assumed to be reversible (i.e., overpotential losses are assumed to be zero). Multiplying Eq. (II.28)by the Avogadro number, N, in order to have molar quantities gives.

$$We,max = nF\Delta Vrev \qquad (II.29)$$

where F is the Faraday number, and $\Delta Vrev$ is the difference between reversible electrode potentials.

The only work forms assumed are the expansion work and electrical work.

$$W = W\,e,max + P\,\Delta V \qquad (II.30)$$

In addition to these, assuming the process is reversible

$$Q = T\Delta S \qquad (II.31)$$

Substituting Eq.(II.29) – (II.31) into Eq.(II.25), the enthalpy change will be

$$\Delta H = T\Delta S - nF\Delta Vrev \qquad (II.32)$$

Eq. (II.32) can be rearranged as follows,

$$\Delta H - T\Delta S = -nF\Delta Vrev \qquad (II.33)$$

where

$$\Delta G = \Delta H - T\Delta S \qquad (II.34)$$

and

$$E = \Delta Vrev \qquad (II.35)$$

Substituting Eqs. (II.34)and (II.33)into Eq. (II.35) gives

$$\Delta G = -nFE \qquad (II.36)$$

E, which is defined as the difference in potentials between the electrodes is called as the electromotive force of the cell (i.e, the reversible potential of the cell, $Erev$). If both the reactants and the products are in their standard states, Eq (II.36) can be written as

$$\Delta G^0 = -nFE^0 \qquad (II.37)$$

where $E°$ is the standard electromotive force, or – as most commonly referred to – is the standard reversible potential of the cell.

II.3.4 Nernst Equation

Let us consider the following reaction,

$$kK + lL \rightarrow mM \qquad (II.38)$$

where k moles of K react with l moles of L to produce m moles of M. Each of the reactants and the products have an associated activity; a_K, and a_L being the activity of the reactants, ; a_M being the activity of the product. For ideal gases, activity term can be written as

$$a = \frac{P}{P_0} \qquad (II.39)$$

p is the partial pressure of the gas, and $p0$ is the pressure of the cell. Eq. (II.22)can be rearranged for the the reaction given in Eq. (II.38), as follows.

$$\Delta\bar{G} = \Delta\overline{G^0} - RT\, ln\left(\frac{a_M^m}{a_K^k\, a_L^l}\right) \qquad (II.40)$$

In the Eq. (II.40), $\Delta\bar{G}$ and $\Delta\overline{G^0}$show the change in molar Gibbs free energy of formation, and the change in standard molar Gibbs free energy of formation. From Eq(II.36), the following relation can be written,

$$E = -\frac{\Delta G}{nF} \qquad (II.41)$$

Substituting Eq. (II.41)into Eq. (II.40)gives the effect on voltage as follows,

$$E = \frac{\Delta\overline{G^0}}{\mathrm{nF}} - \frac{RT}{nF}\, ln\left(\frac{a_M^m}{a_K^k\, a_L^l}\right) \qquad (II.42)$$

Substituting Eq. (II.37)into Eq (II.42)yields,

$$Eo = E^o - \frac{RT}{nF}\, ln\left(\frac{a_M^m}{a_K^k\, a_L^l}\right) \qquad (II.43)$$

where $E°$ is the standard electromotive force, and Eo is defined to indicate the reversible electric voltage. Eq. (II.43)can be rewritten by substituting (II.24)and Eq(II.39), as fo llows.

$$Eo = \frac{RT}{nF} ln\, K - \frac{RT}{nF}\, ln\left(\frac{\left(\frac{P_M}{P_o}\right)^m}{\left(\frac{P_K}{P_o}\right)^k \left(\frac{P_L}{P_o}\right)^l}\right) \qquad (II.44)$$

Eq. (II.43) and (II.44) give the electromotive force in terms of product or/and reactant activity, and is called Nernst equation. The electromotive force calculated using this equation is known as the Nernst voltage, and is the reversible cell voltage that would exist at a given temperature and pressure

II. 4 Water Management

The transport of water within the PEMFC is one of the most important phenomena that directly affects the behavior of the membrane (heart element of the cell). The degree of humidification of the latter is of major importance because of its influence on the efficiency and on the performance of the cell. Water management in PEMFC has become a major concern for researchers and manufacturers because it is a complex issue for which there is no single answer. Indeed, the presence of water is both necessary and harmful to the proper functioning of the cell: a good hydration of the membrane allows better proton conductivity, while too much water vapor can condense and the liquid water thus formed may prevent reagents from reaching the electrodes. To manage this paradox, it is necessary to understand where the water in the heart of the cell comes from and how it can impede its functioning.

Typically, the humidification is applied to the anode and / or cathode inputs to supply water to the membrane region. On the other hand, water is produced at the cathode / membrane interface due to the electrochemical reaction of H + / O2

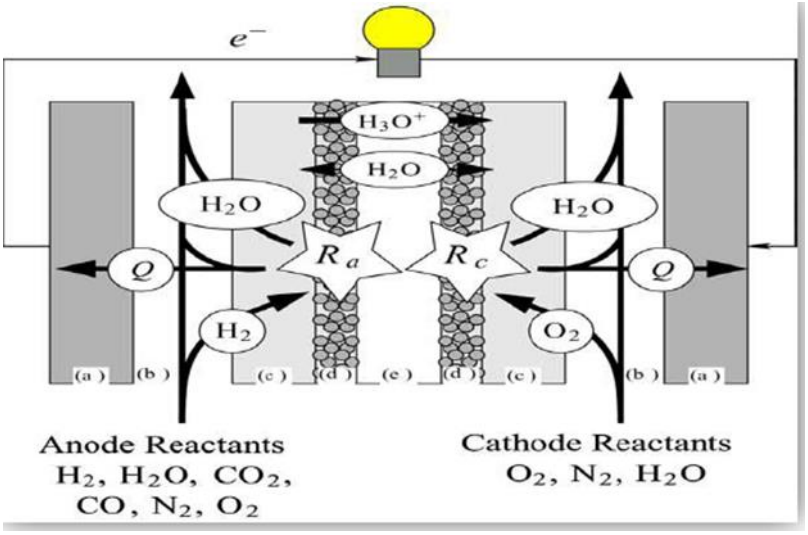

Figure II.1*:* Occurrence processes in a PEM fuel cell. The PEM fuel cell is composed of (a) bipolar plate, (b) gas flow channel, (c) diffusion layer, (d) catalyst layer, and (e) polymer electrolyte layer *[39]*

Les performances de la pile peuvent être affectées par le noyage ou l'assèchement.

II.4.1 Transfers of water in cell

The water present in the cell can have two sources: the humidification of the reactive gases and the cathodic reaction. In a PEMFC, the water is transported in the supply channels, but also through the membrane and the electrodes. We will now take a closer look at the two water transport mechanisms through the membrane shown in Figure (II.2).

Electro-osmosis

Across the membrane, the protons carry with them a number of water molecules. Measurements of the electro-osmosis coefficient (number of water molecules per proton) were carried out on membranes of Nafion117® in a liquid medium at 30 ° C. by Zadowinski et al. (1993) [18]. They observed a linear growth of the electro-osmosis coefficient as a function of the water content λ (number of water molecules per sulphonic site). The water content can be modified by heat treatment of the membrane. Without treatment, when the membrane is in contact with liquid water, λ is classically 22 and the electro-osmosis coefficient is 2.5 H2O / H +. The latter falls to 0.9 for λ equal to 11. in submerged membranes.

Measurements have also been made (Zawodzinski et al ., 1995) [39]in more or less saturated gaseous media, the electro-osmosis coefficient is then constant and equal to 1 for a wide range of values of λ (1.4-14).

Diffusion

The Nafion® membrane can be approximated by a dense medium, that is to say with a compact

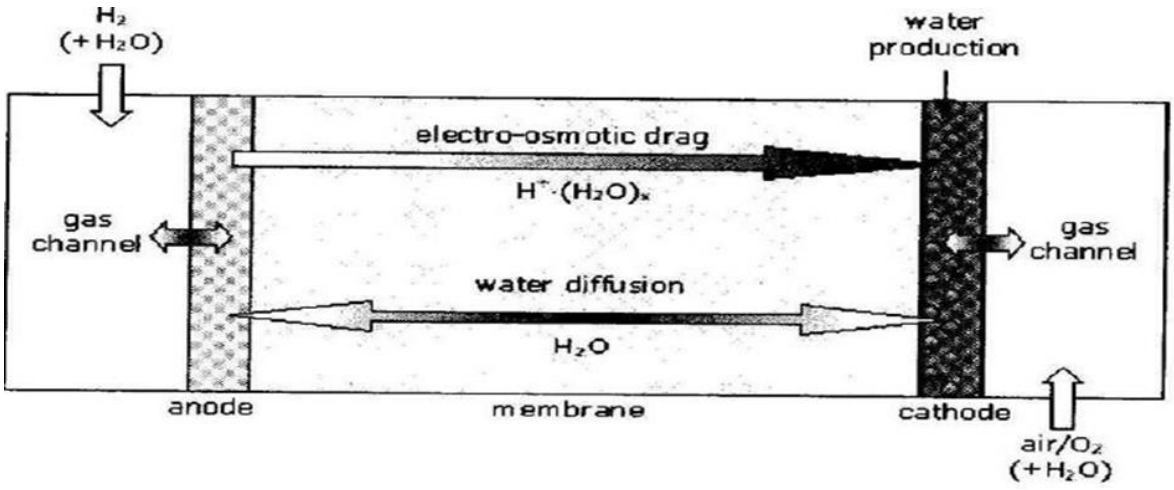

Figure II.2: Mechanisms of water transport in the membrane

structure (non-porous), in which the free spaces between the molecules are of the order of magnitude of the length of the bonds **(Marchand , 1998)** [33].The transport in these dense membranes is done according to 3 stages, sorption of the solute molecules on the upstream face of

the membrane, diffusion of the permeate through the membrane and desorption of the solute from the downstream face of the membrane.

The kinetically limiting step is the diffusion step. The solute diffuses from the most concentrated medium to the most dilute under the influence of a chemical potential gradient. The flow of diffusion through a dense membrane is governed by the law of Fick whose expression can be written:

$$J = -D\frac{\Delta C}{e_m} \qquad (II\ 45)$$

With

J: molar diffusion flux

D: Coefficient of diffusion of water in the membrane,

e_m: Thickness of the membrane,

ΔC: concentration difference across the membrane.

With regard to the flow of water in the electrolyte of the cells, this flow generally takes place from the cathode to the anode. It is even more important that the membrane is thin and that the chemical diffusion coefficient is high.

II.4.2 Effect of operation condition in water management

To avoid of faille in FC according to the improper water management solution such as variety of operating conditions that are suggested by many authors (pressure drop, temperature gradient, control mass flow by compressor, etc.).

II.4.2.1 Humidity

To obtain high performance in FC typically gas inlets are humidified. Buechi and Srinvasan investigated that operation at humidified inlet gases are 40% greater when FC figure out without humidity. Besides, Natarajan and Nguyen declare that with the increasing of humidity at anode side to reduce water transfer due to back-diffusion, going to increase current distribution, etc. [40]

II.4.2.2 Flow rate

in 2008 investigated for air flow rate. Stated that in low flow rate it is beneficial in keeping water in dry cells but will cause of flooding. Hakenjos at al, mentioned FC performance increase (out -put current density higher) with gain flow rate due to higher stoichiometry and the water removed from the flooded cell [41]

II.4.2.3 Temperature

increase temperature leads to increase in saturation pressure and causes evaporation. As a Matter of fact, reduce in flooding will be happened when liquid water diminished. He et al. Investigated of while another operating condition in which (air flow, cell voltage) are constant with increasing temperature from 40 °C to 50 °C causing improvement flooding in the cell [41].

II.4.2.4 Pressure

Electro-osmotic flow rate in normal operating condition is greater than back diffusion flow rate with homogeneous pressure. Wilkinson et al. observed water produced at the cathode side absorbed by the concentration gradient to anode and cause to prevent of flooding. Elevated temperature (evaporation) and gas flow contribute (contribute dissolve water) cause to reduce flooding. However, it cannot be guaranteed drying never happen in the membrane.

II.4.3 Thermal management

Thermal management is an important role to increase/ decrease of performance of the FC.

II.4.3.1 influence of freezing

Freezing can effect on the durability of the FC via thermal and mechanical stress. Decreasing temperature causes to the reduction in proton conductivity of Nafion membrane. Most components that are influenced by freezing temperature such as backing layers, gas diffusion layer and membrane (rarely will be happened because water in membrane strong bond with captions).

II.4.3.2 Start up from freezing

When water at cathode side is not removed during start up with temperature below zero, ice will be covered in surface of GDL and cause to blocking at the catalyst layer. Finally, FC voltage drops and even shuts down FC.

II.4.3.3 Influence high temperature

Performance FC in high temperature has a few benefits such as increase electrochemical kinetics and the result enhance efficiency, advance endurance for contaminants and augments the water management and cooling system.

II.5 Conclusion

In this research work ,The PEMFC modeling and diagnosis are the most important issues treated in literature. A good diagnosis strategy contributes to improve the lifetime of the FC and then to improve the availability of the system built around it, It has been established that the FC is subject to a lot of fault during its operating. The latter are due to multi-physical phenomenon namely the temperature, the pressure and the humidity of the gas involved within the FC stack and cells. Several models have been developed to understand this phenomenon and to evaluate the FC performances according to different conditions of use but also to detect .

The next chapter will Details on the modeling process

CHAPTER III

Mathematical modeling

III.1.Introduction

In a typical PEM fuel cell microchannel, a GDL made of carbon tefloned paper or carbon fabric forms one of the walls, while the other three walls are formed or machined in a bipolar plate made of carbon or metal materials treaties.

This chapter describes a complete, stationary, monophasic model with the flow field in the whole cell of the PEM type with 2D geometry. More precisely, it is a matter of constructing a model that takes into account most of the phenomena interacting within the cell, after a presentation of the structure of the cell, the mass and heat transport equations governing the operation and the different properties of the flow are presented. Through these equations adapted to the model, a presentation of the numerical tool used CFD FLUENT is made.

III.2 Physical Model

The active physical phenomena encountered in the different zones of the stack are: The transport in the continuous and porous media which include the conservation equations (speed, heat, and mass) as well as the empirical relations, with source terms that explain the reactions electrochemical and Joule effect. To be able to build the mathematical model of a planar geometry cell, we first have to define a macroscopic geometrical image, on which we place the coordinate system and define the system of equations composing the model.

III.2.1 Geometry of the modeled structure

The different elements of the model are presented and detailed in this section. The geometry of a PEMFC model cell consists of two cathodic and anodic straight-side flow channels. These channels are separated by two diffusion layers (GDLs) inside which are the so-called active or catalytic reaction zones (CLs) located on either side of a proton exchange membrane or electrolyte, commonly called Membrane-Electrode-Assembly (MEA) as shown in (Figure III.1).

III.2.2 Model assumptions

The determination of a mathematical model of a process generally requires various simplifying assumptions in order to limit its complexity. Our model is based on the following assumptions:

- The cell is powered by wet hydrogen and oxygen.
- The operating state of the cell is stationary.
- The flow in the channels is considered laminar.
- The fluid is incompressible.
- Monophasic model (water in vapor state).
- The gas diffusion layers(GDL), are isotropic materials.

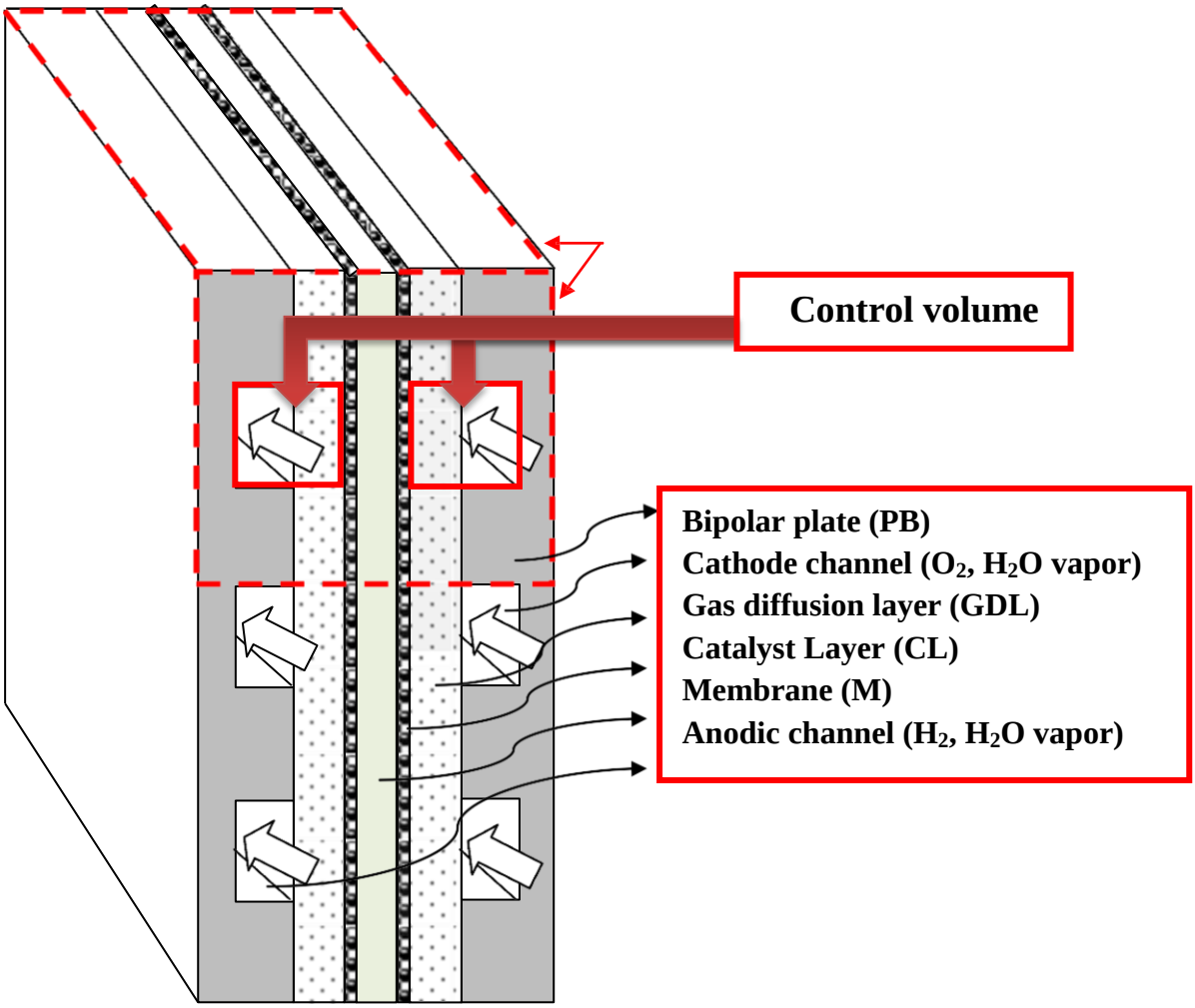

Figure III.1: Presentation of different areas of study of PEMFC.

III.3 Mathematical equations

The transport of the different chemical species must be taken into account in the system of equations describing the dynamics of the fluids in the channels and the porous zones.

The model consists of a single system of nonlinear partial differential equations representing the conservation equations of mass, momentum, continuity, and energy. The conservation equations are written:

❖ **Continuity equation**

The transport of the different chemical species must verify the following continuity equation:

$$\frac{\partial \varepsilon \rho U}{\partial x} + \frac{\partial \varepsilon \rho V}{\partial y} = S_m \qquad (III.1)$$

For all the zones of this model, the term source of mass $S_m = 0$. The porosity **ε** is equal to 1 in the channels.

❖ **Momentum equation**

The fields of velocity and pressure are obtained by the resolution of the equations of motion which are written as follows:

$$U\frac{\partial \varepsilon \rho U}{\partial x} + V\frac{\partial \varepsilon \rho V}{\partial y} = -\varepsilon\frac{\partial \rho}{\partial x} + \frac{\partial}{\partial x}\left(\varepsilon \mu^{eff}\frac{\partial U}{\partial x}\right) + \frac{\partial}{\partial y}\left(\varepsilon \mu^{eff}\frac{\partial U}{\partial y}\right) + S_U \qquad (III.2)$$

$$U\frac{\partial \varepsilon \rho V}{\partial x} + V\frac{\partial \varepsilon \rho V}{\partial y} = -\varepsilon\frac{\partial \rho}{\partial x} + \frac{\partial}{\partial x}\left(\varepsilon \mu^{eff}\frac{\partial V}{\partial x}\right) + \frac{\partial}{\partial y}\left(\varepsilon \mu^{eff}\frac{\partial V}{\partial y}\right) + S_V \qquad (III.3)$$

The source terms S_U , S_V are equal to zero in all zones except for the gas diffusion layers and the catalyst layers model the behavior of the porous medium they are based on Darcy's law.

$$S_U = -\varepsilon\frac{\mu}{K}U \qquad (III.4)$$

$$S_V = -\varepsilon\frac{\mu}{K}V \qquad (III.5)$$

Where: ε: the porosity, K: the permeability of each porous medium of the pile, μ: the viscosity

❖ **Conservation equation of species**

The transport of the different chemical species must be taken into account in the system of equations describing the dynamics of the fluids in the channels and the porous zones. The mass fractions of the different species obey an equation of the same form as the transport equation, or species conservation is necessary to calculate the mass balance for each reagent involved in this model.

$$U\frac{\partial \varepsilon \rho Y_i}{\partial x} + V\frac{\partial \varepsilon Y_i}{\partial y} = \frac{\partial}{\partial x}\left(\rho D_i^{eff}\frac{\partial c_i}{\partial x}\right) + \frac{\partial}{\partial y}\left(\rho D_i^{eff}\frac{\partial U}{\partial y}\right) + S_i \qquad (III.6)$$

Where the index « i ».designates oxygen o_2 on the cathode side and H_2 hydrogen on the anode side and water vapor H_2O vap on both sides.

Where D_i^{eff} and Y_i indicate respectively the effective diffusion coefficients and the molar fractions of the species « i ».

In order to take into account the geometrical constraints of the porous media, the diffusivities are corrected by using the Bruggemann correction formula [24], [42].

$$D_i^{eff} = D_i \, . \, \varepsilon^{1.5} \qquad (III.7)$$

D_i represents the diffusion coefficients of the species « i ».as a function of temperature and pressure is expressed by:

$$D_i = D_i^0 \left(\frac{T}{T^0}\right)^{1.5} \left(\frac{P^0}{P}\right) \qquad (III.8)$$

Three species are taken into account in the calculation of source terms. These are hydrogen (H_2) at the anode, oxygen (O_2), and water vapor (H_2O_{vap}) at the cathode. The source terms S_{H2} and S_{O2} correspond to the decrease in the control volumes relative to the reaction zones of hydrogen and oxygen. The source term of the water S_{H2O} cathode is deduced for it from the source terms S_{H2} and S_{O2}. The variation of species across the reaction zone is dictated by the electrochemical reaction. It is a function that depends only on the current density and is given by Faraday's law

$$S_{i=-\frac{M_i}{nF}i} \qquad (III.9)$$

Where: i is the current density in (A.cm-2), n the number of electrons exchanged during the reaction, F the Faraday constant, MI the molar mass of the constituents « i » in (kg.mol- 1). The chemical reactions of the products and reagents at the cathode and at the anode are respectively:

$$H_2 \rightarrow 2H^+ + 2e^- \qquad (III.10)$$

$$O_2 + 4H^+ + 4e^- = H_2O \qquad (III.11)$$

In the case of the decomposition of hydrogen at the anode, n = 2 in equation (III.10). The term hydrogen consumption is obtained with:

$$S_{H_2=-\frac{M_{H_2}}{2F}i} \qquad (III.12)$$

Oxygen being reduced at the cathode, n = 4 in equation (III.11) and the source term is:

$$S_{O_2=-\frac{M_{O_2}}{4F}i} \qquad (III.13)$$

The amount of water generated at the cathode is given by the following relation:

$$S_{H2O=-\frac{M_{H2O}}{2F}i} \qquad (III.14)$$

Within the catalytic zones, the local current densities i (A.cm-2) are broadly defined as follows [43]:

$$i_a = i_{0,a}^{ref} \left(\frac{C_{H_2}}{C_{H_2}^{ref}}\right)^{1/2} \left[exp\left(\frac{\alpha_a F}{RT}\eta_{act}\right) - exp\left(-\frac{\alpha_c F}{RT}\eta_{act}\right)\right] \quad (III.15)$$

$$i_c = i_{0,c}^{ref} \left(\frac{C_{o_2}}{C_{o_2}^{ref}}\right)^{1/2} \left[exp\left(\frac{\alpha_a F}{RT}\eta_{act}\right) - exp\left(-\frac{\alpha_c F}{RT}\eta_{act}\right)\right] \quad (III.16)$$

Where i: the local current density $ei_{0,a,c}^{ref}$: the reference exchange current density, C: the species concentrations (kg.mol / m3),: the transfer coefficient (dimensionless)).

η_{act} : electrical overvoltage or loss of activation, F: the Faraday constant (C.kg/mol). Equations (III.15) and (III.16) are a general formulation of the Butler-Volmer function. The simplification of this function taking into account the preponderant terms gives the Tafel equations that can still be written:

$$i_a = i_{0,a}^{ref} \left(\frac{C_{H_2}}{C_{H_2}^{ref}}\right)^{1/2} exp\left(\frac{\alpha_a F}{RT}\eta_{act}\right) \quad (III.17)$$

$$i_c = i_{0,c}^{ref} \left(\frac{C_{o_2}}{C_{o_2}^{ref}}\right)^{\frac{1}{2}} exp\left(-\frac{\alpha_c F}{RT}\eta_{act}\right) \quad (III.18)$$

❖ **Energy equation**

It is also important to understand the effects of temperature variation across a fuel cell.

$$(\rho C_P)_{eff}\left(U\frac{\partial T}{\partial x} + V\frac{\partial T}{\partial Y}\right) = \frac{\partial}{\partial x}\left(K_{eff}\frac{\partial T}{\partial x}\right) + \frac{\partial}{\partial y}\left(K_{eff}\frac{\partial T}{\partial y}\right) + S_T \quad (III.19)$$

With: K^{eff} eff the effective thermal conductivity.

The term heat source in the energy equation (III.19) includes:

-The internal heat generation in the fuel cell is the effect of two terms, one of which is due to entropy changes and the other is derived from the heat produced by the activation surge of the reactions in the catalyst [43]:

$$S_T = \left[\frac{T(-\Delta S)}{n\,F} + \eta_{act}\right]_i \quad (III.20)$$

Where: ΔS is the entropy change in chemical reactions, n is the number of electrons and η_{act} is the activation surge.

The heat source associated with the Joule effect is caused by proton transfer resistance in the membrane is given by

$$S_T = \frac{i^2}{\sigma_m} \quad (III.21)$$

Where σ_m:: conductivity of the membrane, expressed as a function of temperature and content ,In λ water, expressed by the correlation suggested by Springer [44], [45].

$$\sigma_{m=(5.139\lambda-3.26)exp\left[1268(\frac{1}{303}-\frac{1}{T})\right]} \quad (III.22)$$

The source terms S_m, S_u, S_v, S_T, S_i are summarized in Table (III.1).

Governing equation	**Volumetric source terms and place of application**
Mass conservation	*For the gas channels, GDL, the anodic and cathodic catalyst layer and the membrane* $S_M = 0$
Conservation of momentum	*For gas channels:* $S_u = S_v = 0$ *For GDLs, CLs and the membrane:* $S_U = -\varepsilon \frac{\mu}{K} U$ $S_V = -\varepsilon \frac{\mu}{K} V$
Energy conservation	*For the gas channels and GDLs:* $S_v = 0$ *For anodic CLs:* $s_T = \eta_{act} . i \frac{i^2}{\sigma_{cat}}$

***Table III.1**: The source terms of the governing equations[45]*

III.4 Numerical simulation

Simulation is defined as the use or resolution of models corresponding to a given system to study the behavior of the latter in a specific context. It is the logical continuation of the modeling which is the first approach of a simulation

III.4.1 Simulation tool (FLUENT ANSYS)

A / Implementation of the model

The implementation of the model in Fluent requires two major steps. The first is to produce the schema and mesh of the cell by using software appropriate to the CFD code. The different areas of the cell are specified by assigning them respectively the appropriate physical characteristics. The

second step is to export the cell schema to Fluent and set the boundary conditions to perform the simulation.

B / Calculation procedure

The calculation procedure requires a certain number of operations in advance of which the overall block diagram is given in Figure (III.2).

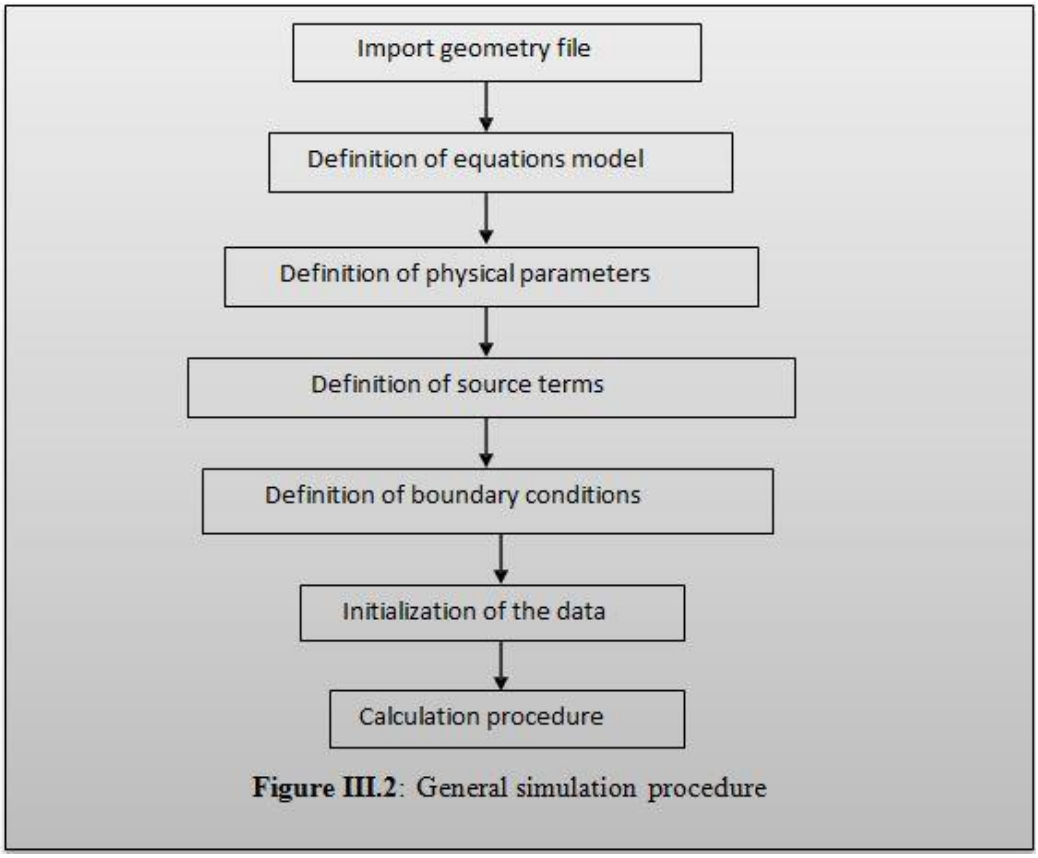

Figure III.2: General simulation procedure

III.4.2 Presentation of the mesh

The mesh that has been used for the domain of modeling is shown in Figure (III.3), the mesh is also built with a high refinement in the gas diffusion layer, because they are very thin. The total number of meshes was approximately (300 × 10000). The solution is considered to be convergent when the relative error of each dependent variable between two iterations

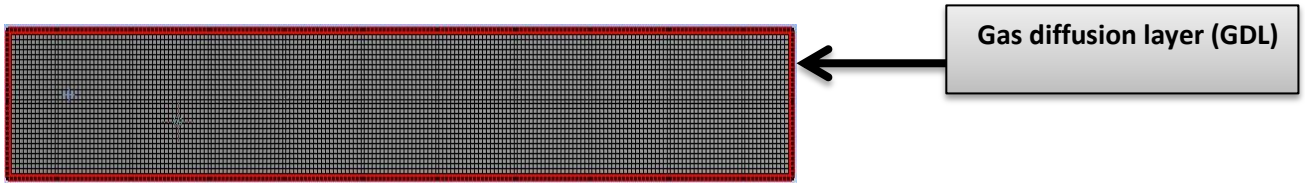

Figure III.3: General presentation of the mesh (GDL)

III.4.3 Boundary conditions

Boundary conditions must be defined for PEM fuel cell simulations, based on the specification of the problem. The definition of the mesh geometry and the boundary conditions were performed, after the mesh was exported to Fluent.

In this model, the boundary conditions were defined as follows:

- in the input areas (massflow type) and output (outflow type) for left anode and cathode gas diffusion layer .

- parois (wall type) représentant des canaux d'anode et de la cathode; ainsi que le collecteur de courant de l'anode et la cathode.

- and the continuity between each component of the gas diffusion layer (interior type).

- walls (axis type) representing anode channels and the cathode; as well as the current collector of the anode and the cathode.

III.5 Modeling parameters

Among the most tedious parts of model development is determining the correct parameters for the model, which will eventually determine the accuracy of the results. All the parameters used for our medializations are listed in the following tables.

III.5.1 Geometric parameters

The geometrical parameters used for the simulations are presented in Table (III.2).

Parameter	symbol	Values	unit	reference
Height of the gas channels	H_{ch}	1×10^{-3}	*(m)*	*[47][34, 46]*
height of anode diffusers, cathode GDL	H_{GDL}	0.3×10^{-3}	*(m)*	*[29]*
Length of anode diffusers, cathode GDL	L_{GDL}	2×10^{-3}	*(m)*	*[29]*
Porosity of the diffusers	ε_{gdl}	*0.4*		*[34, 39, 47, 48][32]*

***Table III.2**: The geometrical parameters used in the model*

III.5.2 Parameters of reaction kinetics

The values of the electrochemical transport parameters are taken from ref. [34]and [49]and are given in Table III.3.

Parameter	symbol	Values	unit	reference
Constant of Faraday	*F*	*96485*	($Cmol^{-1}$)	-
universal constant of gases	*R*	*8.314*	($J.K^{-1}.mol^{-1}$)	-
Coefficient of charge transfer anodic side	a_a	*0.5*	(m^2)	[34]
Load transfer coefficient, cathodic side	a_c	*1*	(m^2/s)	[34]
Exchange current density, anodic side	$i_{0,a}$	1×10^2	(A / m^2)	[49]
Exchange current density, cathodic side	$i_{0,c}$	4×10^{-3}	(A / m^2)	[49]
Limit current	i_L	1.3×10^4	(A / m^2)	-

***Table III.3**: Parameters of reaction kinetics.*

III.5.3 Entry conditions

Table (III.4) gives the input parameters of PEM fuel cell.The values of the operating parameters vary with the case of operation studied but they are specified in the text for each case studied.

Parameter	symbol	Values	unit	reference
Hydrogen and oxygen inlet temperature	T_e	*353*	*(K)*	*[34, 47] [39][32]*
Pressure of the flow channel	P_a , P_c	*101 325*	*(Pa)*	*[33][34, 46, 47]*
Entry speed	U_e	*0.5*	*(m/s)*	-
Molar fraction of hydrogen at the anode	$Y_{H_{2.a}}$	*0.9*	-	-
Molar fraction of water vapor at the anode	$Y_{H_{2.o}vap,a}$	*0.1*	-	-
Molar oxygen fraction at cathode	$Y_{o_{2.c}}$	*0.9*	-	-
Molar fraction of cathode water vapor	$Y_{H_{2.o}vap,c}$	*0.1*	-	-

***Table III.4**: Input parameter*

III.5.4 Material transport parameters

For gas diffusivities in the mass conservation equations given in Table (III.5), experimentally determined values were taken and scaled for temperature and pressure [50].

Parameter	symbol	Values	unit	reference
Electrode permeability	k	1.76×10^{-11}	(m^2)	*[34, 39, 47][32]*
Coefficient of diffusion of H2 in the anode (353 K, 1 atm)	$D^0_{H_2}$	1.1028×10^{-4}	(m^2/s)	*[33]*
Coefficient of diffusion of O2 in the cathode (353 K, 1 atm)	$D^0_{O_2}$	3.2348×10^{-5}	(m^2/s)	*[33]*
Coefficient of diffusion of H2O in the anode (353 K, 1 atm)	$D^0_{H_2O\,.a}$	1.1028×10^{-4}	(m^2/s)	*[33]*
Coefficient of diffusion of H2O in the cathode (353 K, 1 atm)	$D^0_{H_2O\,.c}$	3.8900×10^{-5}	(m^2/s)	*[33]*
Molar mass of hydrogen	M_{H_2}	2×10^{-3}	$(kg\ .mol^{-1})$	
Molar mass of oxygen	M_{O_2}	32×10^{-3}	$(kg.mol^{-1})$	
Molar mass of water	M_{H_2O}	18×10^{-3}	$(kg.mol^{-1})$	

Table III.5: *Transport Parameters Used in the Modeling.*

III.5.5 Definition of material characteristics

The writing of the model requires knowledge of the thermo-physical properties of the different materials constituting the core of the pile, i_e the solid matrix and the nature of the fluid. Fluid characteristics are loaded from the Fluent data library.

The thermal conductivities of bipolar plates (PB), diffusion zones (GDLs) and the membrane are important parameters that greatly influence the temperature fields in the cell. It should be noted that the porous character of the media constituting the cell core (diffusion zone) modifies the thermal transfers within them .

Thus the conductivities used in this model are effective conductivities representing the conductive transfer in the material and in its pores. They are highly dependent on the nature and geometry of the solid matrix, and the nature of the interstitial fluid.

III.5.6 Thermophysical properties

Various models allow the estimation of the effective conductivity of a porous medium from its porosity and the respective conductivities of the solid phase and the fluid phase. The effective conductivity is calculated directly from the law of mixtures:

$$k_{eff} = \varepsilon k_f + (1-\varepsilon)k_s \qquad (III.23)$$

with k_s the conductivity of the solid phase and k_f that of the fluid phase, and ε the porosity of the medium.

The equivalent specific mass specific heat values of the media are also provided for their future transient utility. The equivalent mass heat is calculated directly from the law of mixtures:

$$(\rho C_p)_{eff} = \varepsilon(\rho C_p)_f + (1-\varepsilon)(\rho C_p)_s \qquad (III.24)$$

The equivalent specific heat values of the porous media (the diffusers) and a frame of their effective thermal conductivity are given in the (table III.7).

Fluid	**Density (ρ) (Kg/m)**	**Mass thermal capacity (C_P) (J/Kgk)**	**Thermal conductivity (k) (w\m.k)**	**Viscosity (μ) (kg/ms)**
Hydrogen (H_2)	0.08189	14283	0.1672	8.411×10^{-6}
Oxygen(O_2)	1.2999	919.31	0.0246	1.919×10^{-5}
water vapor(H_2O_{vap})	0.5542	2014	0.0261	1.34×10^{-5}
Water vapor(H_2O_{Liq})	998.2	4182	0.6	0.001003

***Table III.6**: Physical properties of the fluid used in the simulation[39]*

Parameter	***Diffusers (GDL)***		
	By phase		
	Teflon	***H_2***	***O_2***
k (W/ m.K)	*0.15*	*0.1672*	*0.0246*
$\rho C_p (J/Km^3)$	2.2×10^6	1.16×10^3	1.19×10^3
	Pour le milieu		
k_{eff} *(W/ mK)*	*0.15*		
$(\rho C_p)_{eff(J/Km^3)}$	1.32×10^6		

***Table III.7**: Actual thermal conductivities and specific heats of the environments considered.[47].*

III.6 Conclusion

In this chapter we presented the physical model with a general description of these transport equations and momentum to account for flow properties, as well as boundary conditions and different heat source terms in the equation. of energy causing a heating. A simulation tool, the CFD Fluent code was chosen for the resolution of our model and for this, the general synoptic calculation was presented with the thermo-physical properties used. To the knowledge of all these elements combined, the reliable results should be presented by simulation. This is the goal envisioned in the next chapter.

CHAPTER IV

Numerical Simulation of PEMFC using ANSYS FLUENT

IV.1 Introduction

ANSYS Fluent is a state-of-the-art computer program for modeling fluid flow, heat transfer, and chemical reactions in complex geometries.

ANSYS Fluent is written in the C computer language and makes full use of the flexibility and power offered by the language. Consequently, true dynamic memory allocation, efficient data structures, and flexible solver control are all possible. In addition, ANSYS Fluent uses a client/server architecture, which enables it to run as separate simultaneous processes on client desktop workstations and powerful compute servers. This architecture allows for efficient execution, interactive control, and complete flexibility between different types of machines or operating systems.

ANSYS Fluent provides complete mesh flexibility, including the ability to solve your flow problems using unstructured meshes that can be generated about complex geometries with relative ease. Supported mesh types include 2D triangular/quadrilateral, 3D tetrahedral/hexahedral/pyramid/wedge/polyhedral, and mixed (hybrid) meshes. ANSYS Fluent also enables you to refine or coarsen your mesh based on the flow solution.

You can read your mesh into ANSYS Fluent, or, for 3D geometries, create your mesh using the meshing mode of Fluent . All remaining operations are performed within the solution mode of Fluent, including setting boundary conditions, defining fluid properties, executing the solution, refining the mesh, and postprocessing and viewing the results.

In the previous chapter, we presented a stationary monophasic model of a PEM cell with planar geometry. The objective of this chapter is to set up a description of the phenomena of material transport as well as heat in the cell. Only the steady state is considered and the models described are two-dimensional. More precisely, it is a matter of constructing a model that takes into account most of the phenomena interacting within the cell in order to predict the optimal operating conditions for better performances.

IV. 2 Thermal profiles

IV.2.1. Distribution of temperature in the anode gas diffusion layer (GDL)

The distribution of temperature within GDL has important effects on almost all transport phenomena.

Figure (IV.1) shows the distribution and temperature profiles in (K) found by simulation (FLUENT).

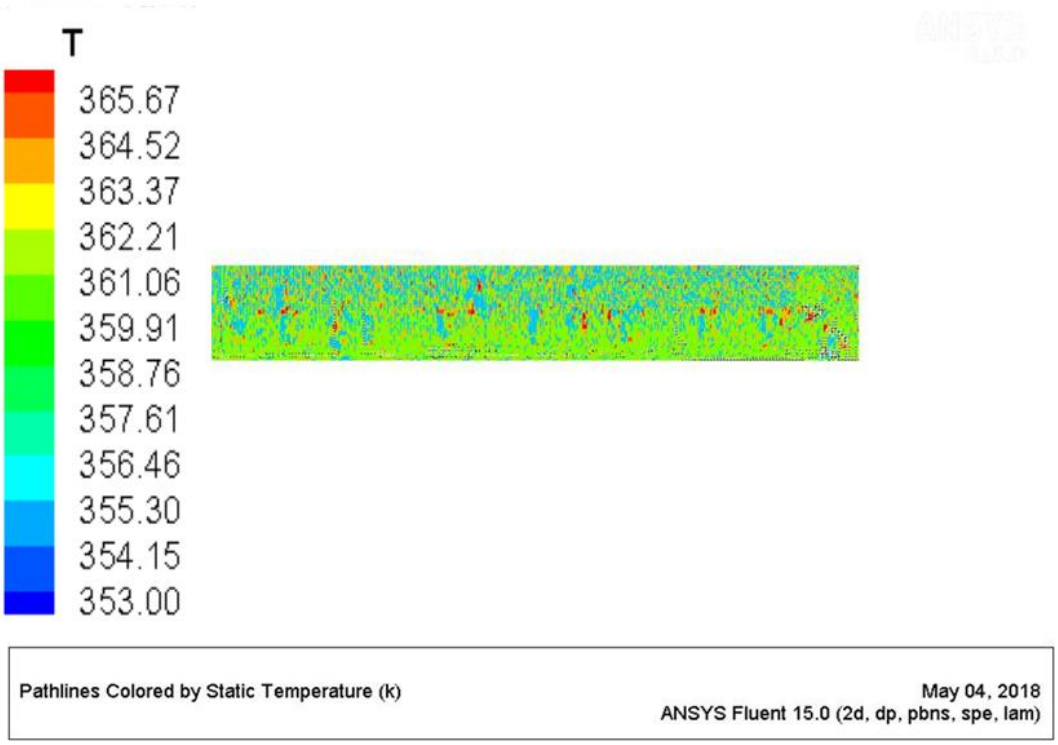

Figure IV.1: Temperature distribution inside GDL(anode)

The results presented showed that the overall level of temperature increase in GDL main zone of diffusion rate production and temperature drop in the channel region. A temperature gradient is minimum of the order of 353 K at a low diffusion rate, and the maximum temperature gradient of 365.67 K at a high diffusion rate

IV.2.2. Distribution of temperature in the cathode gas diffusion layer (GDL)

There is a strong dependence of temperature and current density, this dependence is linked to the

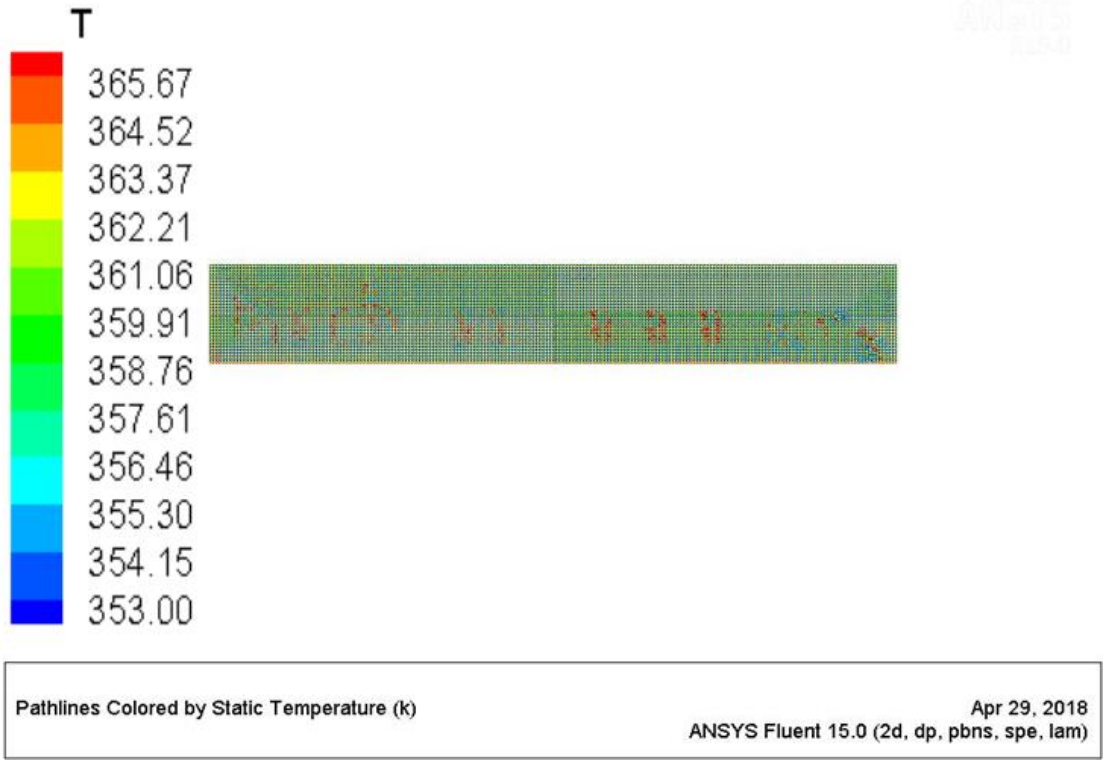

Figure IV.2: Temperature distribution inside GDL(cathode)

physical mechanisms at the origin of the main sources of heat: the speed and mass flow in the cathode. All these phenomena are proportional to the density and mass flow.

IV.3 Distribution of the molar fractions of gases in the gas diffusion layer

IV.3.1 Distribution of the molar fraction of hydrogen

Figure (IV.2) shows the distribution of the molar fraction of hydrogen in the gas diffusion layers in the anode side. In general, the molar fraction of hydrogen decreases from the inlet to the outlet as it is consumed. However, the decrease is quite low along the channel and the decrease in the molar fraction of hydrogen increases under the teeth and the rate of consumption increases the hydrogen fraction reaches zero at the interface of the membrane, which means that all the available hydrogen is exhausted in the thickness of the gas diffusion layer.

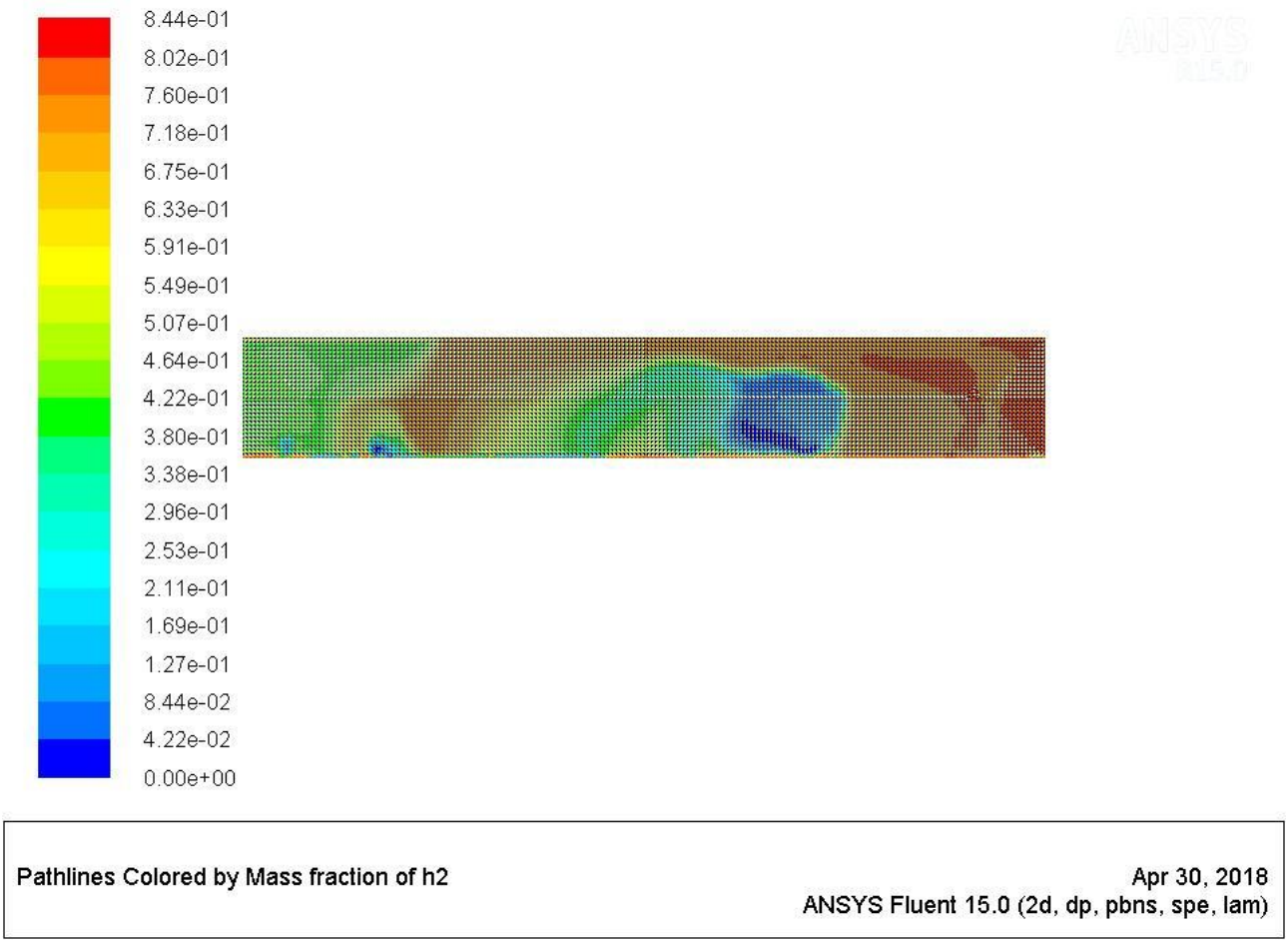

Figure IV.3: Distribution of the molar fraction of hydrogen in the gas diffusion layer

IV.4 Oxygen and hydrogen concentration in the gas diffusion layer GDL

The contour plot of gas concentration of the anode and cathode GDL in Figures (IV.4).(IV.5) shows that there is gas under both the channel and the land for the best performer. This figure also shows that gas is driven towards the catalyst layer by the concentration gradient of gas in the y direction. gas owes through the thickness of the GDL parallel to the y axis and is consumed directly below the channels. In addition, oxygen is also being delivered to the catalyst under the land areas.

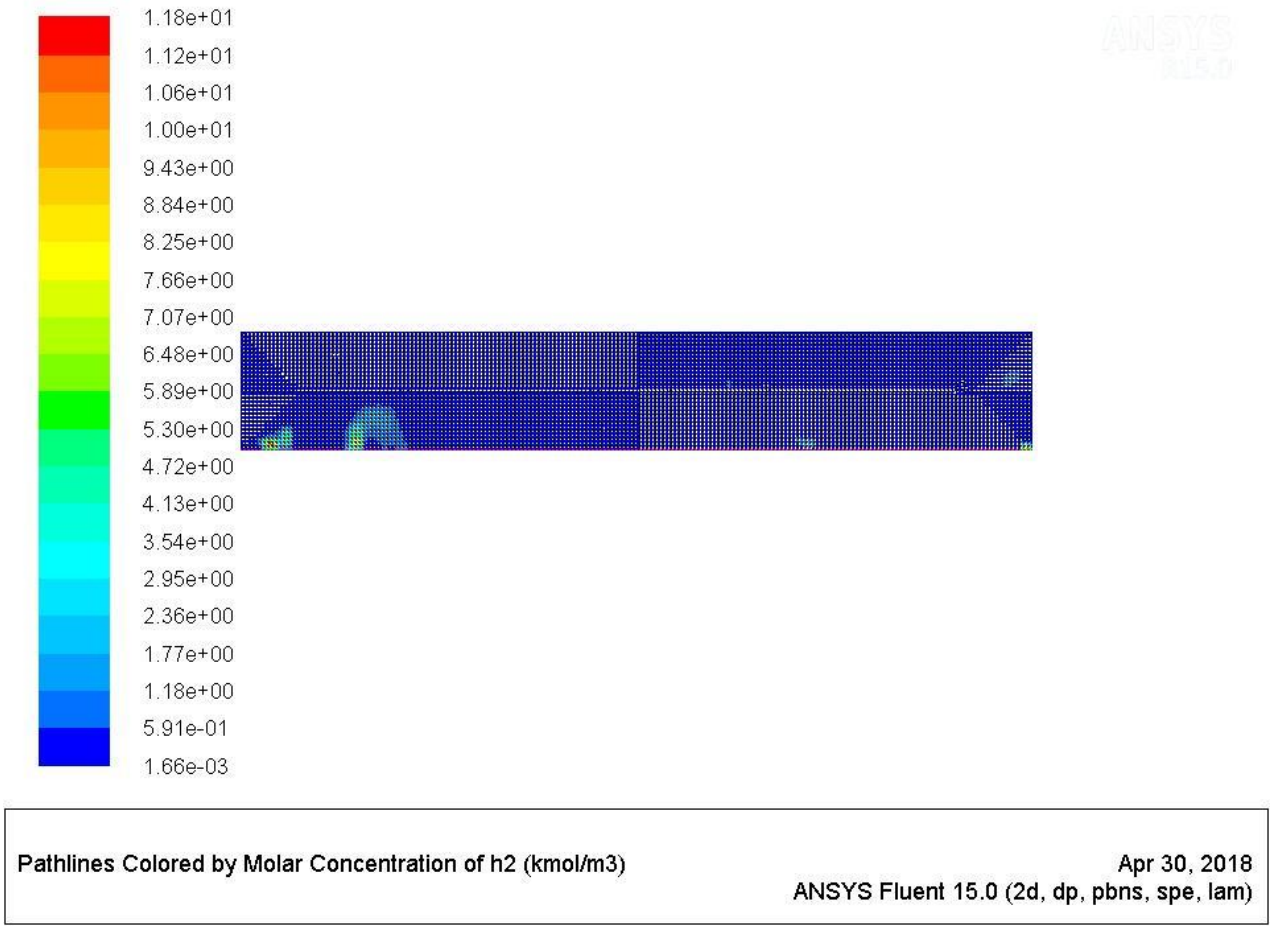

Figure IV.4: Distribution of the molar concentration of hydrogen in the gas diffusion layer

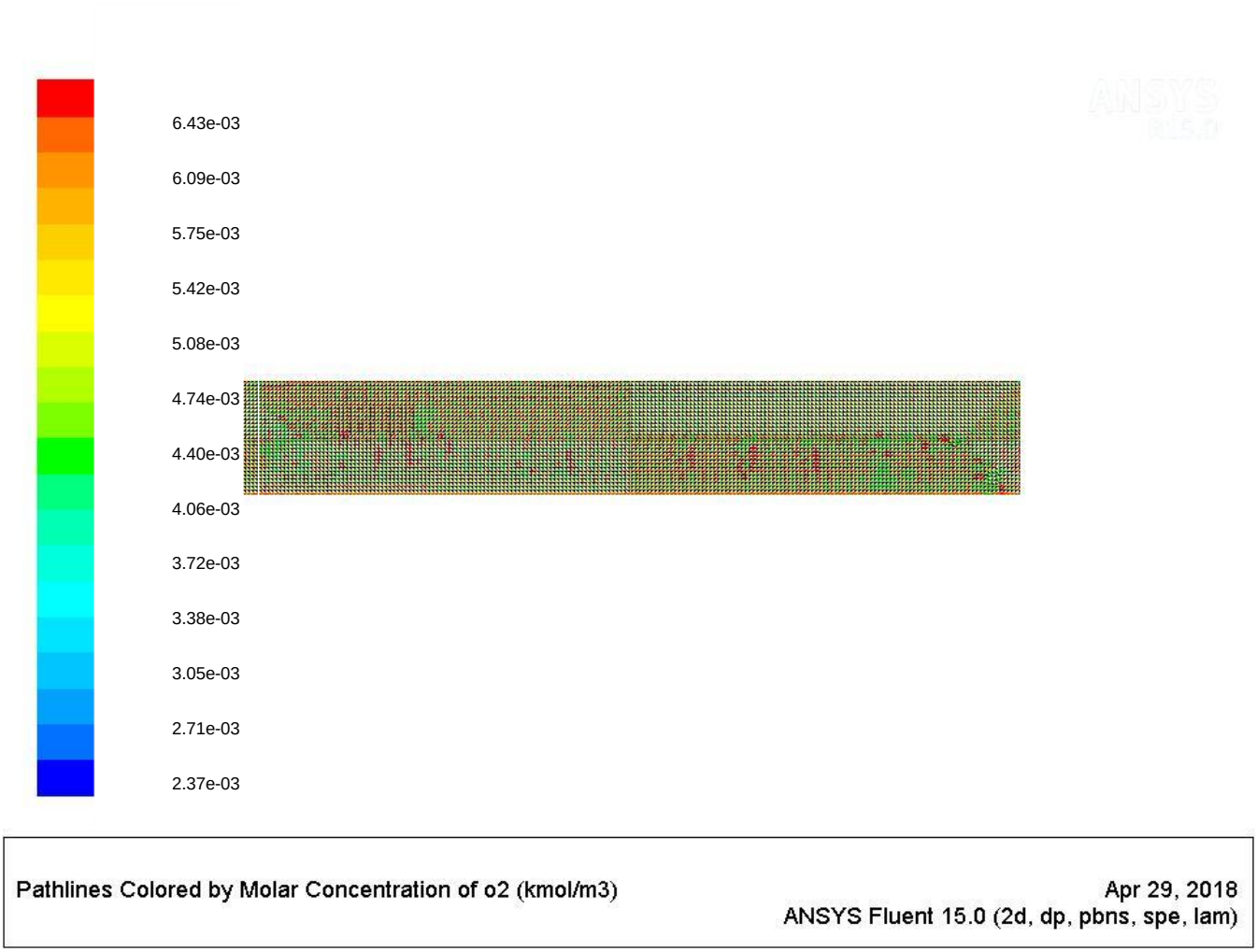

Figure IV.5: Distribution of the molar conentration of oxygen in the gas diffusion layer

Hydrogen is delivered effectively to the catalyst layer even below the land areas. This is a desirable result because all of the catalyst area is able to participate in the reaction. In contrast, the velocities under the channel lands in the case of the worst individual are not very high, implying that diffusion is the dominant transport mechanism for oxygen and hydrogen. And therefore, although the oxygen concentration is high under the channels for the individual, it experiences low oxygen concentration under the channel. Contrary to this result, the best performer shows evidence of both diffusive and convective transport. The absolute pressure distribution within the channels and the GDL provides.

IV.6 Velocity Profile in the gas diffusion layer GDL

The numerical analysis of the velocity distribution along a perforated PEM fuel cell shows that fuel and oxidant follow the shortest possible path from inlet to outlet in the PEM fuel cell gas channel. Results show a high velocity magnitude in gas diffusion layer , possibly leading to dead

zones at the corners of the fuel cell domain. The following figures show the velocity streamlines and velocity vectors along the perforated type PEM fuel cell domain.

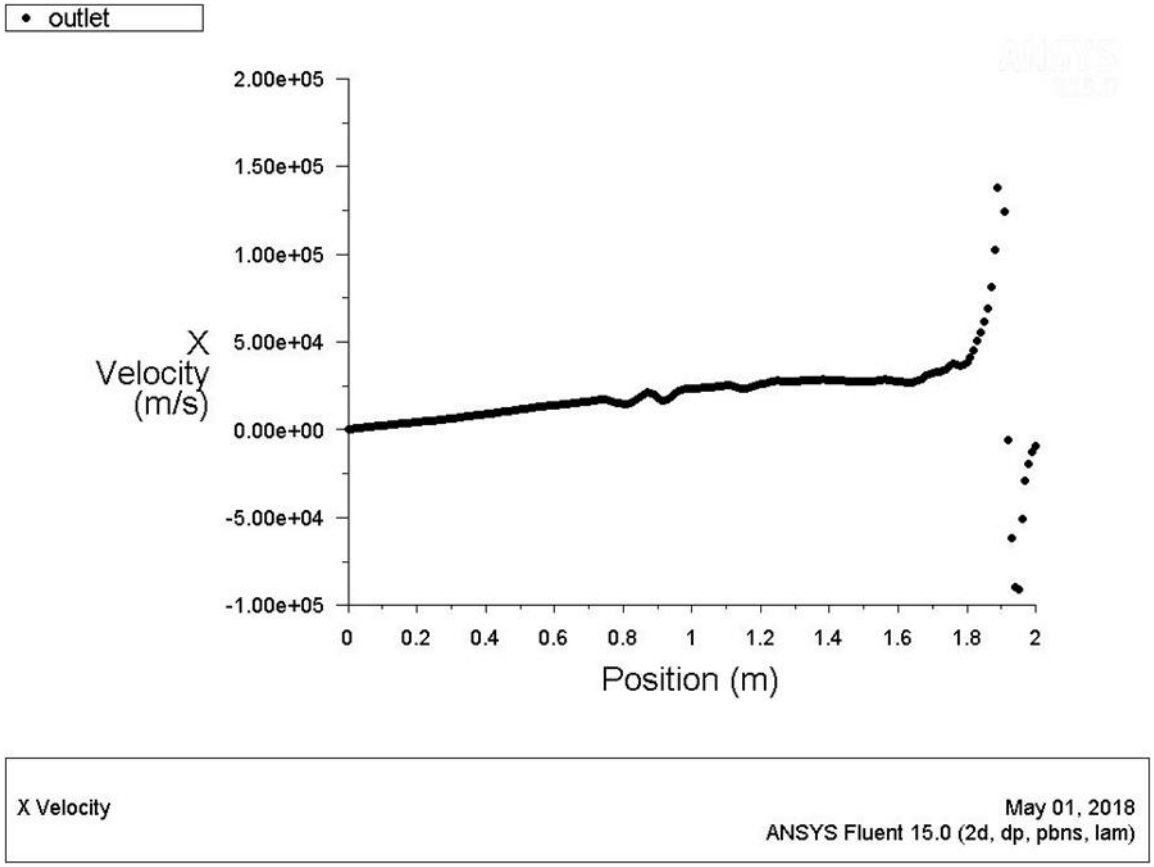

Figure IV.6: the Velocity in the gas diffusion layer

The velocity profile affects the distribution of reactant and product species in the fuel cell domain; therefore, further investigations were carried out to understand and analyses the velocity variation along the gas diffusion layer in the fuel cell. For these analyses, the velocity distribution is studied along a cross-section at the center of the GDL domain.

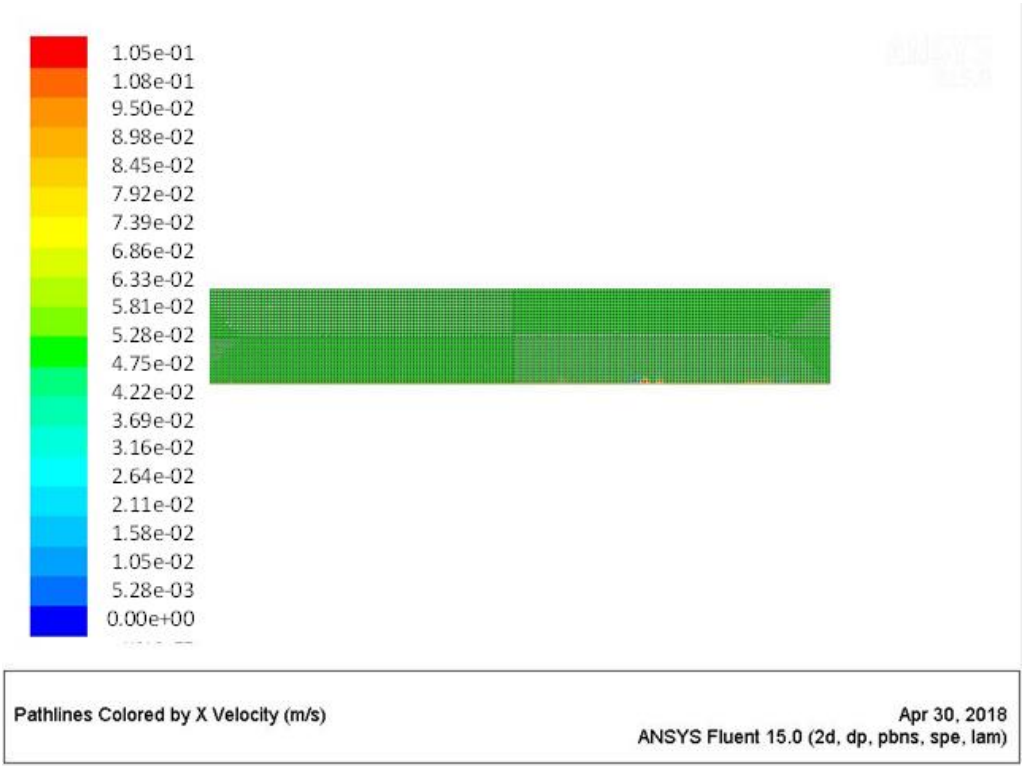

Figure VI.7: Velocity contour in the anode <x>

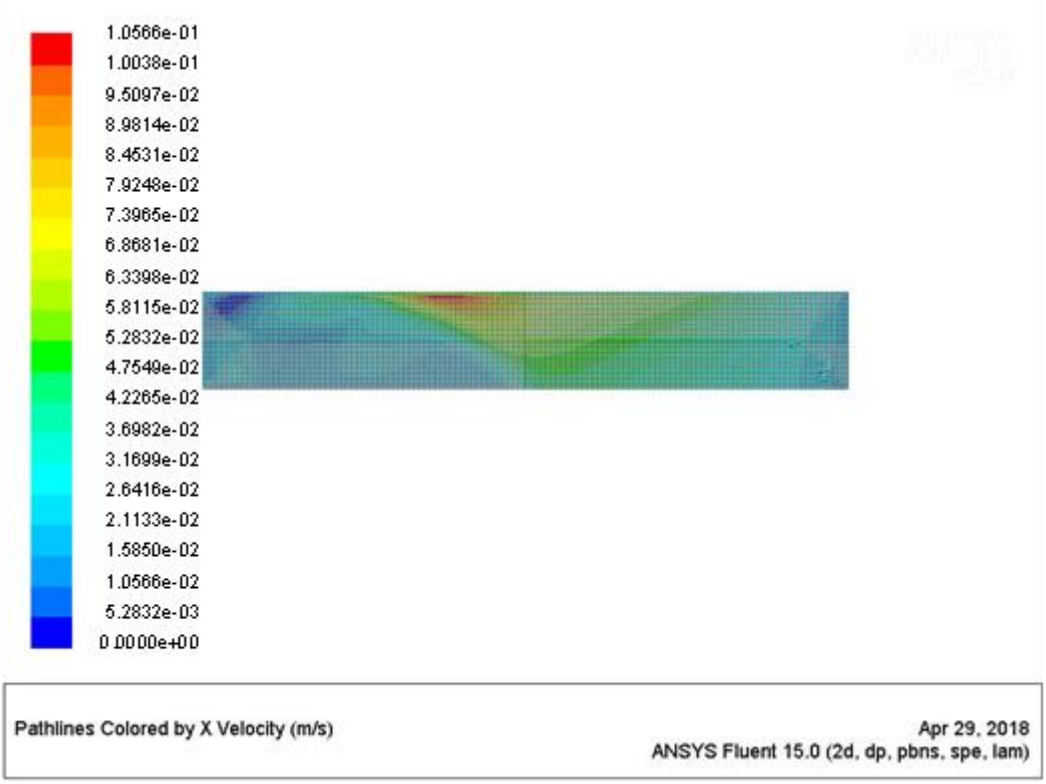

Figure VI.8: Velocity contour in the cathode <x>

The analysis shows a parabolic velocity profile along the cross section, positivity forcing the fuel and oxidant to pass through the perforated holes of the gas distributor. The velocity profile affects the distribution of reactant and product species in the fuel cell domain , therefore, further investigations were carried out to understand and analyses the velocity variation .

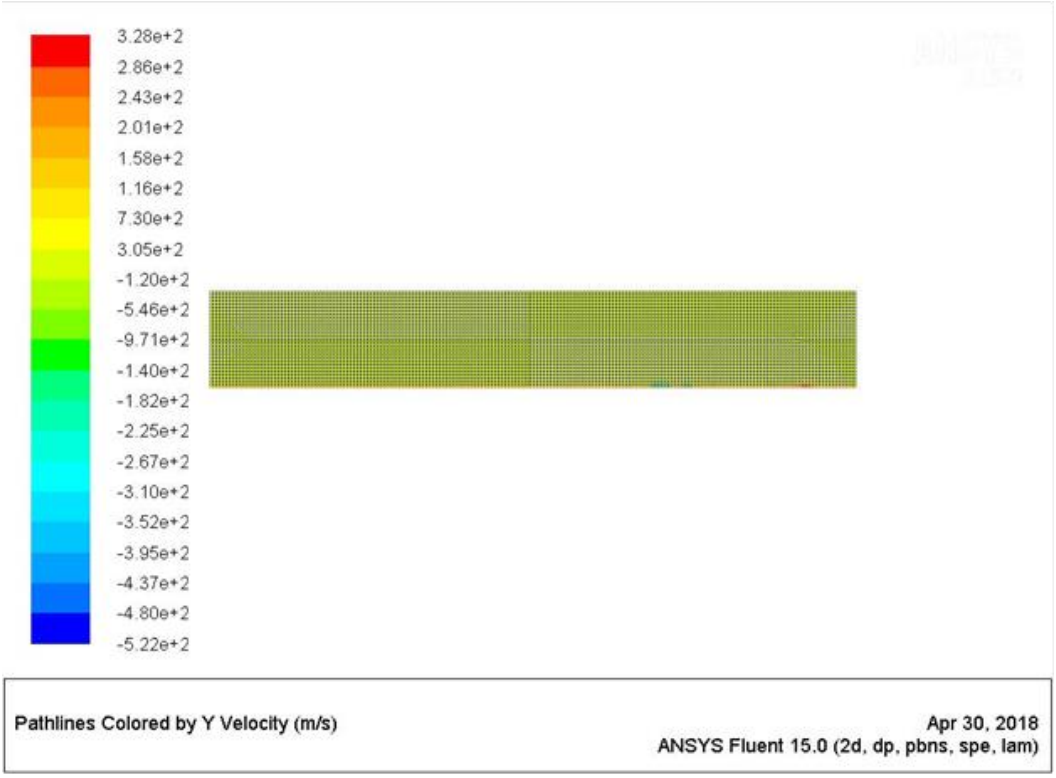

Figure VI.9: Velocity contour in the anode <y>

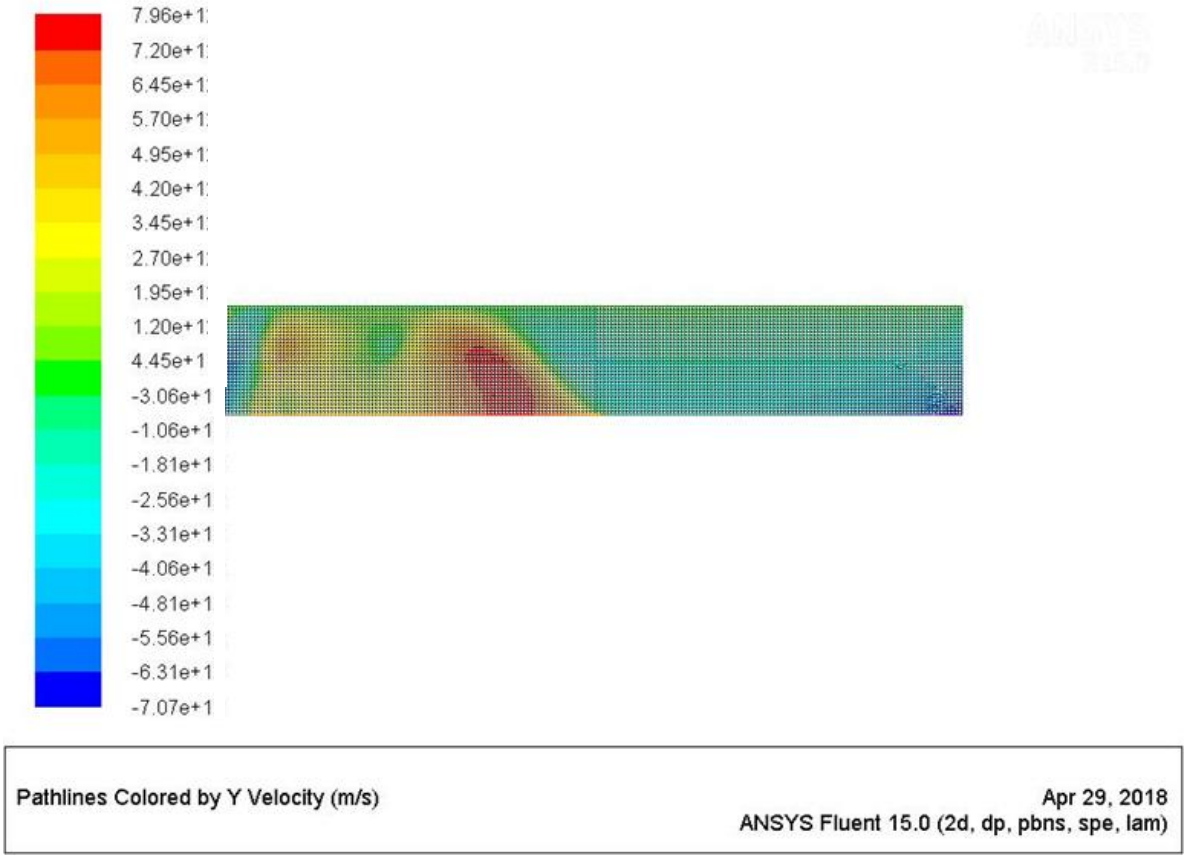

Figure VI.10: Velocity contour in the cathode <y>

The velocity distribution considerably influences the diffusion of reactant species along the gas diffusion layer. For perforated gas flow channels, the reactant flow enters from the inlet and spreads freely out along the gas channel and passes through the perforated holes, whereas in case of serpentine shaped gas channel, the flow is not free to move around. Most of the reactant species get consumed near the inlet section when operating at atmospheric pressure conditions which leads to an uneven distribution of the reactant species along the serpentine PEM fuel cell domain. To overcome such issues, a high pressure flow can be used in a serpentine gas flow channel to move the reactants from the inlet to the outlet; another method is to increase the size of the gas channel, but this can add additional manufacturing costs.

With a decrease in GDL porosity, it becomes increasingly difficult for the reactant species to permeate through the GDL and reach the catalyst region. Therefore, GDL porosity considerably influences the concentration of the reactant species and water flooding characteristics in the PEM fuel cell. Increasing the GDL porosity improves the diffusion of the reactant air through the GDL, which improves the electrochemical reaction rates and the rate of water evaporation from the fuel cell domain.

IV.7 Conclusion

Known limitations of this project include, but are not limited to several important considerations. First, the PEMFC model employed here assumed single- phase ow, which in reality, is incorrect. The production and transport of gas on the cathode and anode, including flooding, is highly relevant for PEMFC performance characterization. Flooding can have a dramatic effect on the reactant gas ow in the cell both in the GDL and in the channel. Multiphase ow was not considered in this PEMFC model in order to reduce model complexity and computational time.

Second, the best individuals tended to consume all of the available reactants before reaching the outlet ports of the cell implying some degree of reactant starvation. These cells could have benefited from a higher inlet mass ow rate such that the reactant utilization was not quite so high, as long as the increased pumping power did not cause the net power density of the cell to drop. While the search spaces explored by this algorithm thus far are useful for lab-scale fuel cell evaluation and comparison, the real value is in the optimization's ability to find an optimal PEMFC design configuration of any size. By successfully demonstrating the optimization of laboratory-scale PEMFCs, the method can confidently be applied to fuel cells of a larger target area. It is expected that in cells with a larger area, the physical mechanisms that govern PEMFC performance would find different optimal parameter values. The method developed here is capable of including as many parameters as a user desires, including varying the material properties. Such additional parameters may include, but are not limited to: channel height, GDL thickness GDL porosity, GDL permeability, channel taper, and the number.

GENERAL CONCLUSION

In this thesis, 2D models, monophasic, stationary of a PEM type cell with planar geometry were studied. The models allow for GDL and gas channels where the flow is perfectly parallel and co-current. The modeling takes into account the transport of material ice the gas phase in the anodic and cathodic diffusers, the channels and the water in the membrane as well as the heat in the whole of the PEM cell (only the steady state is considered). This modeling presents a detailed distribution of reagents, water vapor, temperature field and distribution of heat sources within the gas diffusion layer GDL for different operating and geometrical parameters.

First to third Chapters focused on providing a background on fuel cell concepts as well as the motivations for investigating PEMFCs by means of numerical modeling and simulation. Fuel cells has attracted much attention as a potential power source for portable electronic devices, it is convert the chemical energy of hydrogen and oxygen directly into electricity. Their high efficiency and low emissions have made them a prime candidate for powering the next generation of electric vehicles, and their modular design and the prospects of micro-scaling them have gained the attention of cellular phone and laptop manufacturers .second Chapter focused on the equation numerical method of simulating PEMFC performance. The performance is calculated using a commercially available software package and is meshed appropriately. This third chapter describes a complete, stationary, monophasic model with the flow field in the whole cell of the PEM type with 2D geometry. More precisely, it is a matter of constructing a model that takes into account most of the phenomena interacting within the cell, after a presentation of the structure of the cell, the mass and heat transport equations governing the operation and the different properties of the flow are presented. Through these equations adapted to the model, a presentation of the numerical tool used CFD FLUENT is made. Convergence criteria are discussed in this chapter as well as several types of model verification strategies .

Fourth Chapter is a case study of gas flow in gas diffusion layer. The obtained results aim to understand the different performances of a PEMFC system .

The isothermal analyses show that heat is generated as a by-product of the electrochemical reactions along the gas diffusion layer. Such heat gets distributed along the PEM fuel cell domain and increases the operating Temperature of the PEM fuel cell. Results show that such heat generation is more significant at the cathode and anode side, while at the anode side there is no significant variation in operating temperature, and the temperature remains almost constant .Increasing the GDL porosity improves the efficiency with which the reactant species permeate the GDL. Overall, the performance of the PEM fuel cell increases with an increase in GDL porosity.

Improved knowledge of material properties plays an important role in improving numerical analyses. Material properties of the membrane electrode assembly (GDL), catalyst layer and electrolyte membrane are complex. Continuous research is ongoing by researchers in order to gain improved understanding of the membrane electrode assembly. It is recommended by the author to use this knowledge in developing more comprehensive numerical models of the fuel cell.

Transient numerical analyses are generally more realistic and provide a better picture of the overall scenario. Numerical analyses of the PEM fuel cell with a perforated-type gas distributor were carried out under steady state conditions because the main purpose of this study was to validate the model and analyses.

Bibliographical references

[1] J. Larminie, A. Dicks, and M. S. McDonald, *Fuel cell systems explained*. J. Wiley Chichester, UK, 2003.

[2] M. Dowsett, A. Adriaens, C. Martin, and L. Bouchenoire, "The use of synchrotron X-rays to observe copper corrosion in real time," *Analytical chemistry,* vol. 84, no. 11, pp. 4866-4872, 2012.

[3] A. Dicks and D. A. J. Rand, "Fuel cell systems explained," 2000.

[4] A. R. Balkin, "Modelling a 500W polymer electrolyte membrane fuel cell," *University of Technology, Sydney,* 2002.

[5] S. Haufe and U. Stimming, "Proton conducting membranes based on electrolyte filled microporous matrices," *Journal of Membrane Science,* vol. 185, no. 1, pp. 95-103, 2001.

[6] M. Mikkola, "Experimental studies on polymer electrolyte membrane fuel cell stacks," *Master's thesis submitted in partial fulfillment of the requirements for the degree of Master of Science in Technology, Helsinki University of Technology,* 2001.

[7] M. Mustafa, "Design and manufacturing of a (PEMFC) proton exchange membrane fuel cell," Coventry University, 2009.

[8] K. Kreuer, "On the development of proton conducting polymer membranes for hydrogen and methanol fuel cells," *Journal of membrane science,* vol. 185, no. 1, pp. 29-39, 2001.

[9] B. Smitha, S. Sridhar, and A. Khan, "Solid polymer electrolyte membranes for fuel cell applications—a review," *Journal of membrane science,* vol. 259, no. 1-2, pp. 10-26, 2005.

[10] M. Rikukawa and K. Sanui, "Proton-conducting polymer electrolyte membranes based on hydrocarbon polymers," *Progress in Polymer Science,* vol ,25 .no. 10, pp. 1463-1502, 2000.

[11] V. Mehta and J. S. Cooper, "Review and analysis of PEM fuel cell design and manufacturing," *Journal of Power Sources,* vol. 114, no. 1, pp. 32-53, 2003.

[12] E. Ramunni and M. Kienberger, "Gas-diffussion electrodes for polymeric membrane fuel cell," ed: Google Patents, 2000.

[13] D. Bevers, R. Rogers, and M. Von Bradke, "Examination of the influence of PTFE coating on the properties of carbon paper in polymer electrolyte fuel cells," *Journal of power sources,* vol. 63 ,no. 2, pp. 193-201, 1996.

[14] M. S. Wilson and S. Gottesfeld, "Thin-film catalyst layers for polymer electrolyte fuel cell electrodes," *Journal of applied electrochemistry,* vol. 22, no. 1, pp. 1-7, 1992.

[15] R. Fernandez, P. Ferreira-Aparicio, and L .Daza, "PEMFC electrode preparation: influence of the solvent composition and evaporation rate on the catalytic layer microstructure," *Journal of power sources,* vol. 151, pp. 18-24, 2005.

[16] X. Li and I. Sabir, "Review of bipolar plates in PEM fuel cells :Flow-field designs," *International journal of hydrogen energy,* vol. 30, no. 4, pp. 359-371, 2005.

[17] A. Kumar and R. G. Reddy, "Materials and design development for bipolar/end plates in fuel cells," *Journal of Power Sources,* vol. 129, no. 1, pp. 62-6.2004 ,7

[18] P. L. Hentall, J. B. Lakeman, G. O. Mepsted, P. L. Adcock, and J. M. Moore, "New materials for polymer electrolyte membrane fuel cell current collectors," *Journal of Power Sources,* vol. 80, no. 1-2, pp. 235-241, 1999.

[19] D. S. Watkins, K .W. Dircks, and D. G. Epp, "Fuel cell fluid flow field plate," ed: Google Patents, 1992.

[20] D. S. Watkins, K. W. Dircks, and D. G. Epp, "Novel fuel cell fluid flow field plate," ed: Google Patents, 1991.

[21] M. S. Wilson, "Fuel cell with interdigitated porous flow-field," ed: Google Patents, 1997.

[22] G. Fontès, "Modélisation et caractérisation de la pile PEM pour l'étude des interactions avec les convertisseurs statiques," Institut National Polytechnique de Toulouse, 2005.

[23] W. Tao, C. Min, X. Liu ,Y. He, B. Yin, and W. Jiang, "Parameter sensitivity examination and discussion of PEM fuel cell simulation model validation: Part I. Current status of modeling research and model development," *Journal of power sources,* vol. 160, no. 1, pp. 359-373, 2006.

[24] T. Berning, D. Lu, and N. Djilali, "Three-dimensional computational analysis of transport phenomena in a PEM fuel cell," *Journal of power sources,* vol. 106, no. 1-2, pp. 284-294, 2002.

[25] A. D. Le and B. Zhou, "Fundamental understanding of liquid water effects on the performance of a PEMFC with serpentine-parallel channels," *Electrochimica Acta,* vol. 54, no. 8, pp. 2137-2154, 2009.

[26] J. Baschuk and X. Li, "A general formulation for a mathematical PEM fuel cell model," *Journal of Power Sources* ,vol. 142, no. 1-2, pp. 134-153, 2005.

[27] L. Gerbaux, "Modélisation d'une pile à combustible de type hydrogène/air et validation expérimentale," INP GRENOBLE, 1996.

[28] Z. Wang, C. Wang, and K. Chen, "Two-phase flow and transport in the air cathode of proton exchange membrane fuel cells," *Journal of power sources,* vol. 94, no. 1, pp. 40-50, 2001.

[29] K. W. Lum and J. J. McGuirk, "Three-dimensional model of a complete polymer electrolyte membrane fuel cell–model formulation, validation and parametric studies," *Journal of Power Sources,* vol. 143, no. 1-2, pp. 103-124, 2005.

[30] D. Falcão, P. Gomes, V. Oliveira, C. Pinho, and A. Pinto, "1D and 3D numerical simulations in PEM fuel cells," *international journal of hydrogen energy,* vol. 36, no. 19, pp. 1248.2011 ,12498-6

[31] X. Liu, W. Tao, Z. Li, and Y. He, "Three-dimensional transport model of PEM fuel cell with straight flow channels," *Journal of power sources,* vol. 158, no. 1, pp. 25-35, 2006.

[32] M. Hu, A. Gu, M. Wang, X. Zhu, and L. Yu, "Three dimensional, two phase flow mathematical model for PEM fuel cell: Part I. Model development," *Energy Conversion and Management,* vol. 45, no. 11-12, pp. 1861-1882, 2004.

[33] T. Berning and N. Djilali, "Three-dimensional computational analysis of transport phenomena in a PEM fuel cell—a parametric study," *Journal of Power Sources,* vol. 124, no. 2, pp. 440-452, 2003.

[34] M. A. S. Al-Baghdadi, "Performance comparison between airflow-channel and ambient air-breathing PEM fuel cells using three-dimensional computational fluid dynamics models," *Renewable Energy,* vol. 34, no. 7, pp. 1812-1824, 2009.

[35] B. Laoun, "Simulation of PEMFC performance," *Revue des Energies Renouvelables,* vol. 14, no. 3, pp. 441-448, 2011.

[36] A. M. Bates, *Experimental and analytical study of an open cathode polymer electrolyte membrane fuel cell*. University of Louisville, 2015.

[37] D. Falcão, V. Oliveira, C. Rangel, C. Pinho, and A. Pinto, "Water transport through a PEM fuel cell: A one-dimensional model with heat transfer effects," *Chemical Engineering Science,* vol. 64, no. 9, pp. 2216-2225, 2009.

[38] J. M. Brockris and S. Srinivasan, "Fuel cells: their electrochemistry," 1969.

[39] C.-I. Lee and H.-S. Chu, "Effects of cathode humidification on the gas–liquid interface location in a PEM fuel cell," *Journal of Power Sources,* vol. 161, no. 2, pp. 949-956, 2006.

[40] A. Hakenjos, H. Muenter, U. Wittstadt, and C. Hebling, "A PEM fuel cell for combined measurement of current and temperature distribution, and flow field flooding," *Journal of Power Sources,* vol. 131, no. 1-2, pp. 213-216, 2004.

[41] K. Cooper and M. Smith, "Electrical test methods for on-line fuel cell ohmic resistance measurement," *Journal of Power Sources,* vol. 160, no. 2, pp. 1088-1095, 2006.

[42] P. T. Nguyen, T. Berning ,and N. Djilali, "Computational model of a PEM fuel cell with serpentine gas flow channels," *Journal of Power Sources,* vol. 130, no. 1-2, pp. 149-157, 2004.

[43] M. J. Lampinen and M. Fomino, "Analysis of Free Energy and Entropy Changes for Half-Cell Reactions," *Journal of the Electrochemical Society,* vol. 140, no. 12, pp. 3537-3546, 1993.

[44] T. E. Springer, T. Zawodzinski, and S. Gottesfeld, "Polymer electrolyte fuel cell model," *Journal of the electrochemical society,* vol. 138, no. 8, pp. 2334-2342.1991 ,

[45] T. A. Zawodzinski *et al.*, "Water uptake by and transport through Nafion® 117 membranes," *Journal of the electrochemical society,* vol. 140, no. 4, pp. 1041-1047, 1993.

[46] R. Lemoine-Nava, R. Hanke-Rauschenbach, M. Mangold, and K. Sundmacher" ,The gas diffusion layer in polymer electrolyte membrane fuel cells: A process model of the two-phase flow," *international journal of hydrogen energy,* vol. 36, no. 2, pp. 1637-1653, 2011.

[47] N. Khajeh-Hosseini-Dalasm, K. Fushinobu, and K. Okazaki, "Three-dimensional transient two-phase study of the cathode side of a PEM fuel cell," *international journal of hydrogen energy,* vol. 35, no. 9, pp. 4234-4246, 2010.

[48] H. Meng, "Multi-dimensional liquid water transport in the cathode of a PEM fuel cell with consideration of the micro-porous layer (MPL)," *international journal of hydrogen energy,* vol. 34, no. 13, pp. 5488-5497, 2009.

[49] C.-Y. Jung, C.-H. Park, Y.-M. Lee, W.-J. Kim, and S.-C. Yi, "Numerical analysis of catalyst agglomerates and liquid water transport in proton exchange membrane fuel cells," *international journal of hydrogen energy,* vol. 35, no. 16, pp. 8433-8445, 2010.

[50] G. H. Guvelioglu and H. G. Stenger, "Computational fluid dynamics modeling of polymer electrolyte membrane fuel cells ",*Journal of Power Sources,* vol. 147, no. 1-2, pp. 95-106, 2005.

[51] http://www.fctec.com/fctec_types_pafc.asp.

[52] http://www.fctec.com/fctec_types_mcfc.asp

Thesis title:. Contribution to the Simulation of Coupled Transfers Phenomenon Application on the PEM Fuel Cell

Master : Energetic

Authors: FERDJANI Abdelfettah / YAHIA Abdennour.

Abstract:

The interest of clean environmentally friendlier and more efficient energy sources leads to the increase of interest in fuel cells, as it has no production other than water and heat. Fuel cells are electrochemical devices that are designed to directly convert, with high efficiency, the chemical energy from the reaction of the fuel (hydrogen in case of PEMFC) and an oxidant (oxygen) into electricity. In the proton exchange membrane (PEM) fuel cell study, numerical analysis of complex and coupled multi-disciplinary processes involving the subjects of fluid dynamics, heat transfer, mass transport, and electrochemistry has been attempted over the past few decades. However, the performances of the PEMFC can improve by the development of the used models and the obtained results

Key words: CFD Fluent; Fuel cell; Modeling; Simulation; GDL.

Résumé

L'intérêt de sources d'énergie propres, plus respectueuses de l'environnement et plus efficaces, conduit à un intérêt accru pour les piles à combustible, car il n'y a pas d'autre production que l'eau et la chaleur. Les piles à combustible sont des dispositifs électrochimiques qui sont conçus pour convertir directement, avec un rendement élevé, l'énergie chimique provenant de la réaction du combustible (hydrogène dans le cas de PEMFC) et d'un oxydant (oxygène) en électricité. Dans l'étude des piles à combustible à membrane échangeuse de protons (PEM), l'analyse numérique de processus complexes et multi-disciplinaires couplés impliquant la dynamique des fluides, le transfert de chaleur, le transport de masse et l'électrochimie a été tentée ces dernières décennies. Cependant, les performances de la PEMFC peuvent s'améliorer par le développement des modèles utilisés et des résultats obtenus.

Mots clés : CFD Fluent; Pile à combustible ; Modélisation ; GDL.

ملخص:

إن الاهتمام بمصادر الطاقة النظيفة الصديقة للبيئة الأكثر كفاءة يؤدي إلى زيادة الاهتمام بخلايا الوقود ، حيث لا يوجد لديها إنتاج غير الماء والحرارة. خلايا الوقود هي أجهزة كهروكيميائية تم تصميمها للتحويل المباشر ، بكفاءة عالية ، الطاقة الكيميائية من تفاعل الوقود (الهيدروجين في حالة PEMFC) والأكسدة (الأكسجين) إلى كهرباء. في دراسة خلايا الوقود بغشاء التبادل البروتوني (PEM) ، تمت محاولة التحليل العددي للعمليات المعقدة والمتعددة الاختصاصات التي تشمل مواضيع ديناميكية السوائل ، ونقل الحرارة ، والنقل الجماعي ، والكيمياء الكهربائية على مدى العقود القليلة الماضية. ومع ذلك ، يمكن لأداء PEMFC تحسين من خلال تطوير النماذج المستخدمة والنتائج التي تم الحصول عليها.PEMFC

الكلمات المفتاحية : CFD ; خلية وقود ; النمذجة ; المحاكاة ; GDL